Geol. Mag. **153** (*5/6*), *2016, pp. 1166–1191.* © *Cambridge University Press 2016*
doi:10.1017/S0016756816000637

The role of basement-involved normal faults in the recent tectonics of western Taiwan

KENN-MING YANG*†, RUEY-JUIN RAU*, HAO-YUN CHANG*, CHING-YUN HSIEH*‡, HSIN-HSIU TING*§, SHIUH-TSANN HUANG§, JONG-CHANG WU§ & YI-JIN TANG*

*Department of Earth Sciences, National Cheng Kung University, 1 University Road, Tainan 701, Taiwan
‡Oil and Gas E&P Department, Formosa Petrochemical Corporation, 201 Dun Hua N Road, Taipei 105, Taiwan
§Exploration and Development Research Institute, CPC Corporation, 1 Ta Yuan, Wen Fa Road, Wen Sheng, Miaoli 36042, Taiwan

(*Received* 24 November 2015; *accepted* 3 June 2016; *first published online* 5 August 2016)

Abstract – In the foreland area of western Taiwan, some of the pre-orogenic basement-involved normal faults were reactivated during the subsequent compressional tectonics. The main purpose of this paper is to investigate the role played by the pre-existing normal faults in the recent tectonics of western Taiwan. In NW Taiwan, reactivated normal faults with a strike-slip component have developed by linkage of reactivated single pre-existing normal faults in the foreland basin and acted as transverse structures for low-angle thrusts in the outer fold-and-thrust belt. In the later stage of their development, the transverse structures were thrusted and appear underneath the low-angle thrusts or became tear faults in the inner fold-and-thrust belt. In SW Taiwan, where the foreland basin is lacking normal fault reactivation, the pre-existing normal faults passively acted as ramp for the low-angle thrusts in the inner fold-and-thrust belt. Some of the active faults in western Taiwan may also be related to reactivated normal faults with right-lateral slip component. Some main earthquake shocks related to either strike-slip or thrust fault plane solution occurred on reactivated normal faults, implying a relationship between the pre-existing normal fault and the triggering of the recent major earthquakes. Along-strike contrast in structural style of normal fault reactivation gives rise to different characteristics of the deformation front for different parts of the foreland area in western Taiwan. Variations in the degree of normal fault reactivation also provide some insights into the way the crust embedding the pre-existing normal faults deformed in response to orogenic contraction.

Keywords: inversion tectonics, normal fault reactivation, foreland tectonics, fold-and-thrust belt, western Taiwan.

1. Introduction

In the outer part of most of mountain belts, several factors, such as lithology of sedimentary rocks that are deformed in the fold-and-thrust belt, basement morphology of foreland basin, mechanical property of thrust sheets, lithosphere rheology and slip rate of thrusting, are known to cause various styles of frontal thrusts (Morley, 1986; Vann, Graham & Hayward, 1986; Dunne & Ferrill, 1988; Mouthereau, Watts & Burov, 2013). In some cases, such as the tectonic environment of pre-orogenic rifted continental margin characterized by array of the basement-involved normal faults and basement highs, stresses induced by arc-/continent-continent collision could transmit far beyond the mountain front (Letouzey, 1986), cause the pre-existing tectonic settings to be reactivated and form high-angle thrusts or strike-slip faults (Sengor, 1976; Sengor, Burk & Dewey, 1978; Jackson, 1980; Cohen, 1982; Brown, 1984; Etheridge, Branson & Sturt-Smith, 1985; Letouzey, 1986; Harding & Tuminas, 1988; Cooper & Williams, 1989; Coward, 1994; Buchanan & Buchanan, 1995; Lacombe & Mouthereau, 2002; Butler, Tavarnelli & Grasso, 2006; Nemčok, Mora & Cosgrove, 2013), influencing foreland tectonics and thus shaping characteristic tectonic trends and structural styles of the belt front (Welbon & Butler, 1992; Macedo & Marshak, 1999; Lacombe *et al.* 2003; Marshak, 2004; Yang *et al.* 2006; Butler, Tavarnelli & Grasso, 2006). Variations in trends of the pre-existing normal fault with respect to the maximum compressional stress induced by crustal contraction cause various amounts and types of reactivated or inverted normal faults (Etheridge, Branson & Stuart-Smith, 1985; Sassi *et al.* 1993). The style and the extent to which the pre-existing normal faults are involved in the orogenic belt would also determine the estimation of shortening across the deformed terranes (Mouthereau *et al.* 2001; Lacombe & Mouthereau, 2002; Butler, Tavarnelli & Grasso, 2006; Mouthereau & Lacombe, 2006; Carola *et al.* 2013; Carrera & Muñoz, 2013; Jimenez *et al.* 2013; Moreno *et al.* 2013; Tesón *et al.* 2013).

In the young and active tectonic belt of Taiwan, the geological records in the foreland area, including the Western Foothills and the foreland basin offshore and onshore western Taiwan, not only reveal the early

†Author for correspondence: kmyang@mail.ncku.edu.tw

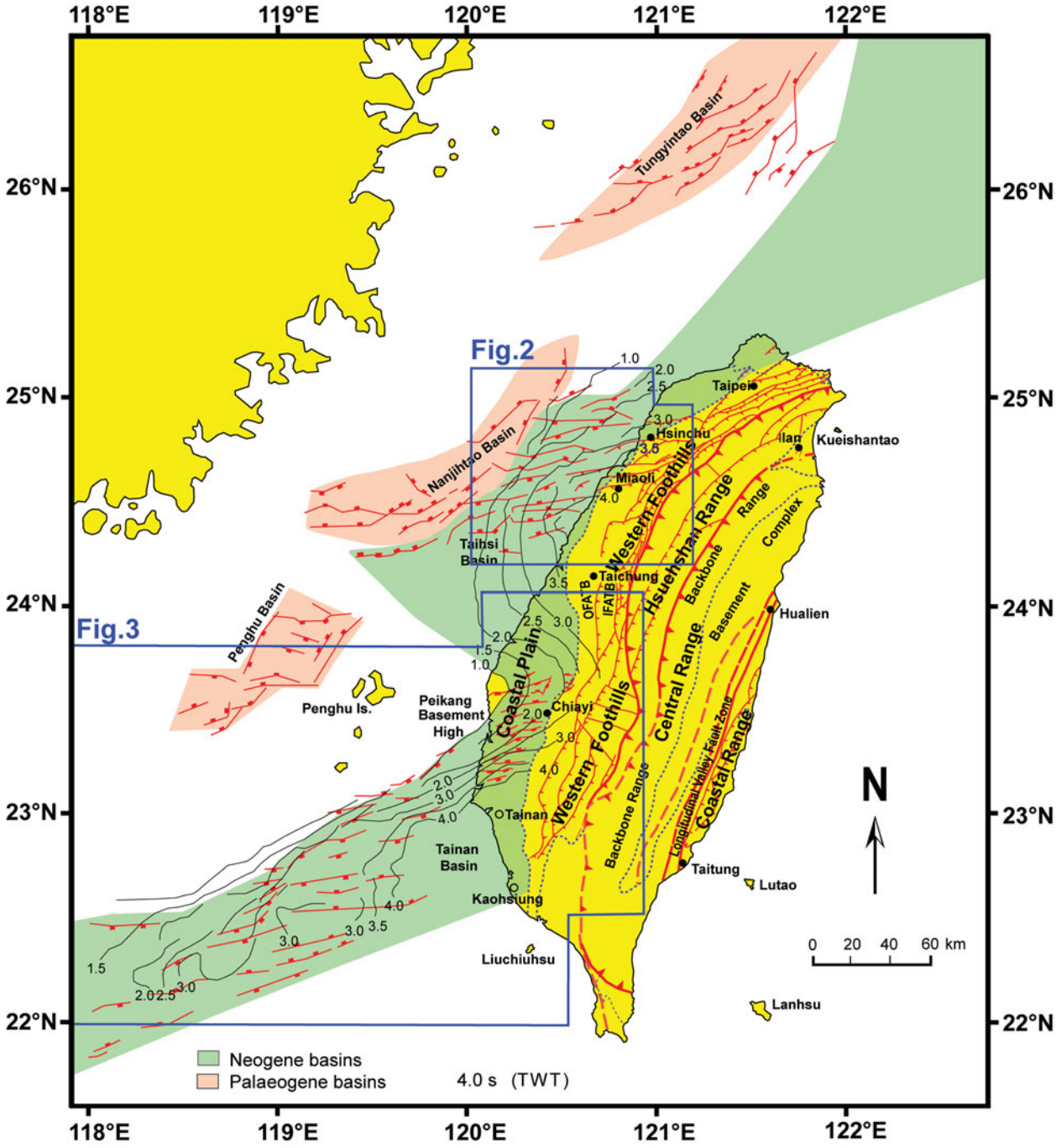

Figure 1. Tectonic map of Taiwan and its adjacent areas (from Yang *et al.* 2006). In this paper, the foreland areas cover the Taihsi and Tainan basins, the Peikang Basement High and the outer and inner fold-and-thrust belts (OFATB and IFATB). The horizon of time contours is a regional unconformity separating the Palaeogene and Neogene rifted basins.

evolutionary history of the foreland itself but also provide key insights into thrust kinematics during mountain belt development. Taiwan is located at the convergent plate boundary between the Eurasia and Philippine Sea plates, and is one of the most active orogenic belts in the world caused by arc-continent collision (Biq, 1972; Chai, 1972; Tsai, 1978; Teng & Wang, 1981) with a converging rate of 70 km Ma^{-1} (Seno, 1977; Suppe, 1984; Seno, Stein & Gripp, 1993). Before the orogeny, western Taiwan was located on the rifted passive margin and encountered at least two phases of early–middle Cenozoic rifting (Sun, 1982; J. Yuan et al., unpub. report, 1989; Lin, Watts & Hesselbo, 2003; Yang *et al.* 2006). The youngest pre-orogenic extensional phase began by middle–late Miocene time (Hsiao, 1974; Tang, 1977; Sun, 1982; Leu, Chiang & Huang, 1985; Chow, Yuan & Yang, 1986; Chow, Yang & Chen, 1987, 1988; Yang, Ting & Yuan, 1991; Yuan *et al.* 1988; J. Yuan et al., unpub. report, 1989; Lin, Watts & Hesselbo, 2003) and formed two eastwards wide-opened rifted basins, the Tainan and Taihsi basins (Fig. 1), which are separated by the Peikang Basement High standing nearly perpendicular to the front of the thrust belt (Sun, 1982; Yang, Ting & Yuan, 1991; Yang

https://doi.org/10.1017/S0016756816000637 Published online by Cambridge University Press

et al. 2006). Since the initiation of orogeny at 7.1–4 Ma (Chi, Namson & Suppe, 1981; Teng, 1990; Huang *et al.* 1997; Huang, Yuan & Tsao, 2006; Mesalles *et al.* 2014), the entire mountain belt has gradually migrated westwards (Chi, Namson & Suppe, 1981; Suppe, 1981) while cannibalizing the pre-orogenic sequences accumulated in the sedimentary basins located on the margin of the Eurasian Plate (Covey, 1984; Teng, 1990).

Several models have been proposed to describe the kinematics and deformation mechanisms in arc-continent collision (Suppe, 1984; Teng, 1990; Sibuet & Hsu, 1997; Lee *et al.* 2015), and they all refer to pre-orogenic basin architecture. The geometry of the geological structures of the basement highs and basement-involved normal faults which coexisted with the pre-orogenic sedimentary basins had a great influence on the spatial and temporal distribution of structural styles in the mountain belt (Meng, 1962, 1967; Chiu, 1970, 1971; Huang, 1986, 1987; Biq, 1992; Lu, 1994; Lu & Malavielle, 1994; Lu *et al.* 1998; Yang *et al.* 1997; Lacombe *et al.* 2001, 2003; Mouthereau *et al.* 2002). While some previous studies regarded the mountain belt in western Taiwan as a typical thin-skinned fault-and-thrust belt (Chiu, 1970, 1971; Suppe, 1976, 1980; Suppe & Namson, 1979; Namson, 1981, 1983, 1984; Hung & Wiltschko, 1993; Hung *et al.* 1999; Hickman *et al.* 2002), a few reactivated high-angle normal faults have been described in the deformation belt (Namson, 1981; Suppe, 1984, 1986; Brown *et al*. 2012; Alvarez-Marron *et al*. 2014). The effects of the pre-existing normal faults on the development of the fold-and-thrust belt have been investigated and evaluated in order to explain the complexity of geological structures in the outer part of the belt (Lee *et al.* 1993; Yang *et al.* 1994, 1996, 1997; Mouthereau *et al.* 2001, 2002; Lacombe & Mouthereau, 2002; Lacombe *et al.* 2003). Some previous studies depicted the major thrusts as the high-angle reactivated normal faults in Western Foothills and insist that the fold-and-thrust belt there has been primarily shaped by thick-skinned deformation (Chang *et al.* 1996; Mouthereau *et al*. 2001; Lee, Chang & Coward, 2002). Lately, the thin- and thick-skinned models seem to be reconciled that all the reactivated normal faults in NW Taiwan are regarded as parts of the imbricate system and share a common décollement in the basement of the fold-and-thrust belt (Lacombe & Mouthereau, 2002; Mouthereau *et al.* 2002). In our previous studies (Yang *et al.* 1996, 1997, 2006), we suggested that pre-existing normal faults have been selectively reactivated and interacting with low-angle thrust faults that were developed by thin-skinned process, and that their effects and occurrences in the Western Foothills and foreland basin should be confined to a limited extent.

The aforementioned various models indicate that the role of pre-existing basement-involved normal faults in the mountain-building process is still controversial and three key issues remand to be addressed. First, the pre-orogenic tectonics in the foreland area of the Taiwan Strait and western Taiwan is characterized by at least two phases of rifting. The normal faults which formed during the oldest phase and led to the opening of the South China Sea have been regarded as those reactivated latterly in the Western Foothills and Hsueh-shan Range (Yue, Suppe & Hung, 2005; Mouthereau & Lacombe, 2006; Brown *et al*. 2012; Alvarez-Marron *et al*. 2014). Reactivation of the normal faults that were formed during the younger phase of rifting has received less attention, except for that mentioned in Yang *et al.* (1994). In the following we will demonstrate that the latter is more important than, or at least as important as, the former in shaping the foreland tectonics in western Taiwan. Second, the general trend of pre-existing normal faults is oblique to that of the orogenic belt, and the kinematics of interaction between pre-existing normal faults and low-angle thrusts in such a situation has been seldom addressed. Third, tectonic implications of variations in structural style and active tectonics related to normal fault reactivation along the strike of the fold-and-thrust belt need to be unravelled to infer inhomogeneity of crustal/lithospheric deformation, as addressed by Mouthereau *et al*. (2002). Yang *et al*. (2006) provided a thorough review on the studies of foreland tectonics in western Taiwan. Based on the previous results and some extra new data, this paper revisits some of the key structural settings in the foreland of western Taiwan and aims to reassess the role of pre-existing basement-involved normal faults in the development of recent tectonics. After providing detailed descriptions and discussing these, we comment on the applicability of various proposed tectonic models on the orogeny of Taiwan.

2. Regional geology and tectonics

2.a. Tectonic compartments

The tectonics in offshore and onshore western Taiwan are characterized by the structures of the pre-orogenic extensional tectonics and those of the outer fold-and-thrust belt that mingle with normal fault reactivation of the syn-orogenic tectonics (Fig. 1). Through the entire offshore western Taiwan, a regionally widespread unconformity corresponding to strata of upper Eocene – lower Oligocene age divides the Cenozoic basin system into Palaeogene and Neogene basins (Sun, 1982; Lin, Watts & Hesselbo, 2003; Yang *et al*. 2006). In the western part of the Taiwan Strait, the Palaeogene basins are half-grabens lining up in a left-lateral en échelon NE–SW trend, covered by thin Neogene and younger strata. In the eastern part of the strait, the Palaeogene basins have been overprinted by younger rift structures and covered by thick sediments in the Neogene basins. While the northwestern margin of the Neogene rift basins also strike NE–W, the single normal faults in the basins are E–W- to ENE–WSW-striking (Fig. 1; Sun, 1982; Yang, Ting & Yuan, 1991; Huang, Chen & Chi, 1993).

Tectonically, onshore Taiwan can be divided into five geological provinces (Fig. 1; Ho, 1986; Huang *et al.* 2001): (1) the Coastal Range, composed of terranes of

https://doi.org/10.1017/S0016756816000637 Published online by Cambridge University Press

accreted volcanic island to the orogenic belt during the collision (Huang, Yuan & Tsao, 2006); (2) the Central Range, characterized by metamorphic complex (schists in the eastern limb, the Basement Complex) and accreted terranes (slates in the western limb, the Backbone Range) (Huang *et al*. 1997; Beyssac *et al*. 2007); (3) the Hsuehshan Range, formerly an Early Cenozoic graben formed in the continental margin and later accreted to the orogenic belt during the collision (Teng *et al*. 1991); (4) the Western Foothills, the fold-and-thrust belt containing sedimentary sequences deposited in the passive margin and then in the foreland basin settings (Suppe, 1981; Yang *et al*. 2006); and (5) the Coastal Plain in the central and southwestern parts of the island, the nearly undeformed foreland area. All these provinces are usually separated by large-scale thrusts or strike-slip faults.

The structures in the Western Foothills, which are mainly addressed in this paper, are generally characterized by unmetamorphosed deformation, open folding and imbricate thrust sheets (Ho, 1982; Suppe, 1985). The tightness of folds decreases from east to west in the foothills belt, which indicates that the magnitude of deformation decreases toward the west (Namson, 1981, 1983, 1984). The deformation front of the Western Foothills in northwestern Taiwan is now around the coastal line (Fig. 2).

2.b. Characteristics of the pre-Neogene basement in the foreland

The pre-Neogene basement and its characteristics have been defined and discussed in Mouthereau *et al.* (2002) and Yang *et al.* (2006). Well-bore data in the foreland areas of western Taiwan reveal that the pre-Neogene basement is not metamorphosed but more compacted than the overlying Neogene sedimentary rocks (Huang, 1967; Leu, Chiang & Huang, 1985; Fuh, 2000; Yang *et al.* 2014) and its top has been regarded as the décollement below the fold-and-thrust belt in some balanced cross-sections across the Western Foothills (Suppe & Namson, 1979; Namson, 1981, 1983, 1984; Hung & Wiltschko, 1993; Yang *et al.* 2007; Brown *et al*. 2012; Alvarez-Marron *et al*. 2014). Stratigraphic sections based on well-bore data also show that the age of the basement rocks underlying the regional unconformity ranges from Mesozoic to Eocene across the basin (Yang *et al.* 2006); only one deep well bore penetrates the Palaeozoic crystalline limestone in the subsurface of coastal plain in southwestern Taiwan (Jahn, Chi & Yui, 1992). The amount of erosion corresponding to the unconformity is up to 3500 m in the basement high, an estimate based on sonic transit time log (Fuh, 2000), indicating that significant uplifting would have brought deeply seated rocks upwards in contact with much younger strata at shallow depth. The normal faults discussed in this paper all cut through the regional unconformity, and can therefore be defined as basement-involved normal faults (Leu, Chiang & Huang, 1985; J. Yuan et al., unpub. report, 1989; Yang, Ting & Yuan, 1991; Yang *et al.* 2006, 2014; Lin, Watts & Hesselbo, 2003).

2c. Fault structures in the foreland

Fault structures in the foreland of offshore and onshore western Taiwan can be grouped into three types: a high-angle normal fault; a high-angle thrust fault with or without significant strike-slip component; and a low-angle thrust fault. The first and second types are the normal faults formed during the youngest rift tectonics and the reactivated tectonics, respectively. The low-angle thrust faults are the major thrusts in the fold-and-thrust belt of Western Foothills. Distribution and intersecting relationships among these fault types can be shown in the tectonic maps depicting the detailed fault structures (Figs 2, 3).

In the Neogene Taihsi Basin of offshore northwestern Taiwan, the distribution and strike of the two types of high-angle fault are not uniform but vary in some spatial characteristics (Fig. 2). In the westernmost part of the basin, almost all normal faults still have their original attitude and sense of slip (Fig. 2; Huang, 1986; Huang, Chen & Chi, 1993). In the area closer to the coastal line, some normal faults have been inverted as high-angle thrusts with a strike-slip component (Huang, 1986; Huang, Chen & Chi, 1993). In this area normal faults and high-angle thrusts are alternatively distributed, but the high-angle thrusts appear more often in the eastern part of the faults of long lateral length in the eastern part of offshore the Taihsi Basin. Most of the faults are mainly striking in a range from N60° E to N100° E. There are also some fault segments striking N30° E. It is noticeable that some faults with main N60° E to N100° E strike extend onto the onshore area and connect with, or are parallel to, the exposed faults that mainly strike N70° E to N90° E.

In the onshore area, the Western Foothills can be divided into the outer and inner fold-and-thrust belts (Ho, 1982) with a boundary along the Chuhuangkeng anticline, the Fangpokeng anticline (Peipu-Chutung thrust) and the Juanchiao thrust (Fig. 2). The trends of the anticlines and thrust faults in the outer fold-and-thrust belt are not uniform and can be grouped into two sets (Fig. 2). In the eastern part of the area that is adjacent to the Chuhuangkeng anticline, the trends of the anticlines and the associated low-angle thrust faults, including the Paoshan (Hsincheng thrust), Yunghoshan (Luchukeng thrust) and Chinshui anticlines, are mostly NNE–SSW, parallel to that of the mountain range which is ranging from N30° E to N60° E. In the western part of the area, which is adjacent to the coastal line, the high-angle faults and the accompanied anticlines, including the Chingtsaohu, Chiting, Chunan, Paishatun and Sanhu anticlines, are striking N70° E to N90° E, parallel to the high-angle normal faults, non-reactivated and reactivated, in the offshore area but at a high angle to the general trend of the orogenic belt. The high-angle faults segment the low-angle thrusts and the accompanied anticlines in the outer fold-and-thrust belt are

https://doi.org/10.1017/S0016756816000637 Published online by Cambridge University Press

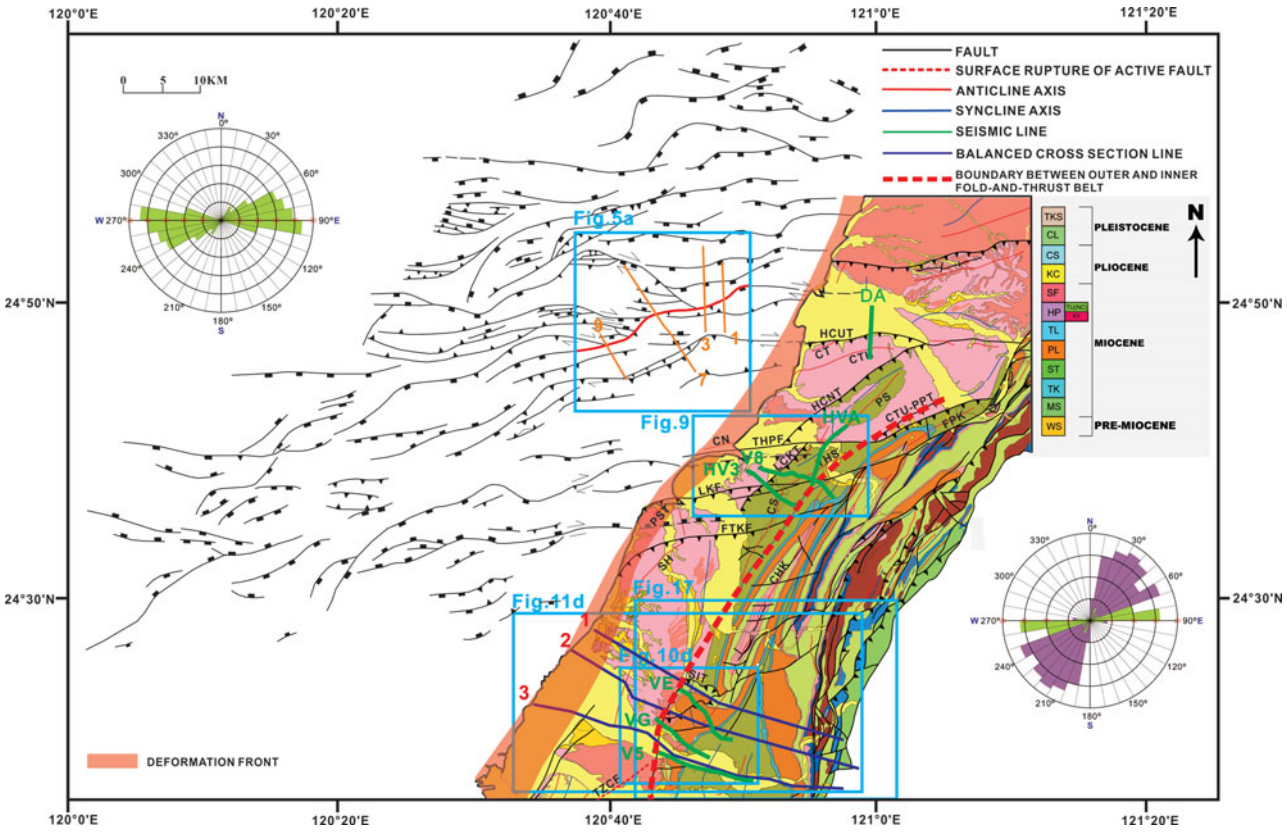

Figure 2. Tectonic map of northwestern Taiwan showing spatial distribution of various types and regional trends of all faults (compiled and modified from Huang, Chen & Chi, 1993 and Chinese Petroleum Corporation, 1978, 1994). The rose diagrams in the upper left and lower right represent regional trends of faults in offshore and onshore areas, respectively. The locations of faults in offshore area are from the contours of the Miocene top. The trends of faults in onshore area are divided into groups of that trending E–W (green) and that trending NE–SW (purple). See the discussions of their tectonic meaning in the text. HCUT – Hsinchu thrust; HCNT – Hsincheng thrust; CTU-PPT – Chutung-Peipu thrust; THPF – Touhuanping fault; LCKT – Luchukeng thrust; LKF – Lungkang fault; FTKF – Futoukeng fault; SIT – San-I thrust; TZCF – Tunzuchiao Fault. Anticlines: CHK – Chuhuangkeng; PS – Paoshan; YHS – Yunghoshan; CS – Chinshui; CTH – Chingtsaohu; CT – Chiting; CN – Chunan; PST – Paishatun; SH – Sanhu.

cut off by the thrust faults in the inner fold-and-thrust belt to the east.

In the Neogene Tainan Basin, offshore southwestern Taiwan, all the faults are high-angle normal faults striking from N70° E to N90° E (Fig. 3) in contrast with that in offshore northwestern Taiwan (Fig. 2). In the coastal plain area most normal faults are E–W-striking. Some normal faults and a few normal fault-inverted thrusts in the frontal area of the fold-and-thrust belt are striking N10° E to N40° E. The normal faults in the coastal plain area extend to the east and are cut off by the low-angle frontal thrust of the Western Foothills.

3. Structural styles of normal fault reactivation

In western Taiwan, normal fault reactivation can be manifested by fault plane geometry of reactivated single normal faults and interaction between reactivated normal faults and low-angle major thrusts. The structural styles of normal fault reactivation are demonstrated in the seismic and balanced cross-sections. Abbreviations used for the formations and faults in the interpreted sections are listed in Figure 4 and Table 1, respectively.

3.a. Reactivation of single normal faults

This paper uses a grid of seismic sections and well-bore data to constrain strata on both sides of reactivated normal faults and to reconstruct geometry of a fault plane (Figs 2, 5a) in the northeastern margin of the Taihsi Basin. Thickening of sedimentary strata in the hanging wall of a high-angle thrust indicates that a high-angle normal fault (F3-E) has been partially reactivated as a high-angle thrust (Fig. 5b). To the west, the upper part of the N-dipping fault plain is rotated and replaced by a S-dipping high-angle thrust (F3) (Fig. 5c). Further westwards, the inversion displacement is transferred southwards to another S-dipping high-angle thrust (F1) (Fig. 5d). The displacement along the high-angle thrust is the largest in the middle part of the fault plane (Fig. 5d) and decreases laterally to its ends (Fig. 5e), where the fault still maintains normal fault displacement.

Similar structural styles associated with reactivation of single normal faults can be observed in onshore northwestern Taiwan. Most of them have been documented in Yang *et al.* (1996, 1997) and cited in Lacombe & Mouthereau (2002) and Lacombe *et al.* (2003) to propose their basement-involved tectonic

https://doi.org/10.1017/S0016756816000637 Published online by Cambridge University Press

Table 1. Faults within the Western Foothills of Taiwan

Study area	Seismic sections	Balanced cross-sections	Faults (abbreviations)
NW Taiwan	Lines 1, 3, 5–7, 9, DA, HVA, V8, HV3, VE, VG, V5	Lines 1–3	Hsinchu thrust (HCUT), Lungkang fault (LKF), Touhuanping fault (LKF), Hsincheng thrust (HCNT), Luchukeng thrust (LCKT), Hsiaonanshih fault (HNSF), San-I thrust (SIT), Tunzuchiao fault (TZCF), Hsinkai fault (HKF), Tamaopu fault (TMPF), Changhua thrust (CHT)
Central Taiwan		Lines 4–6	Changhua thrust (CHT), Chelungpu thrust (CLPT), Hsiaomao thrust (HMT), Tsukeng thrust (TKT), Shuilikeng thrust (SLKT)
SW Taiwan	VA, V1, GB, GA	Lines 7–10	Chiuchiungkeng thrust (CCKT), Chukou thrust (CKT), Tachienshan thrust (TCST), Pinlangchai thrust (PLCT), Luku thrust (LKT), Lunhou thrust (LHT), Matoushan thrust (MTST), Meishan fault (MSF)

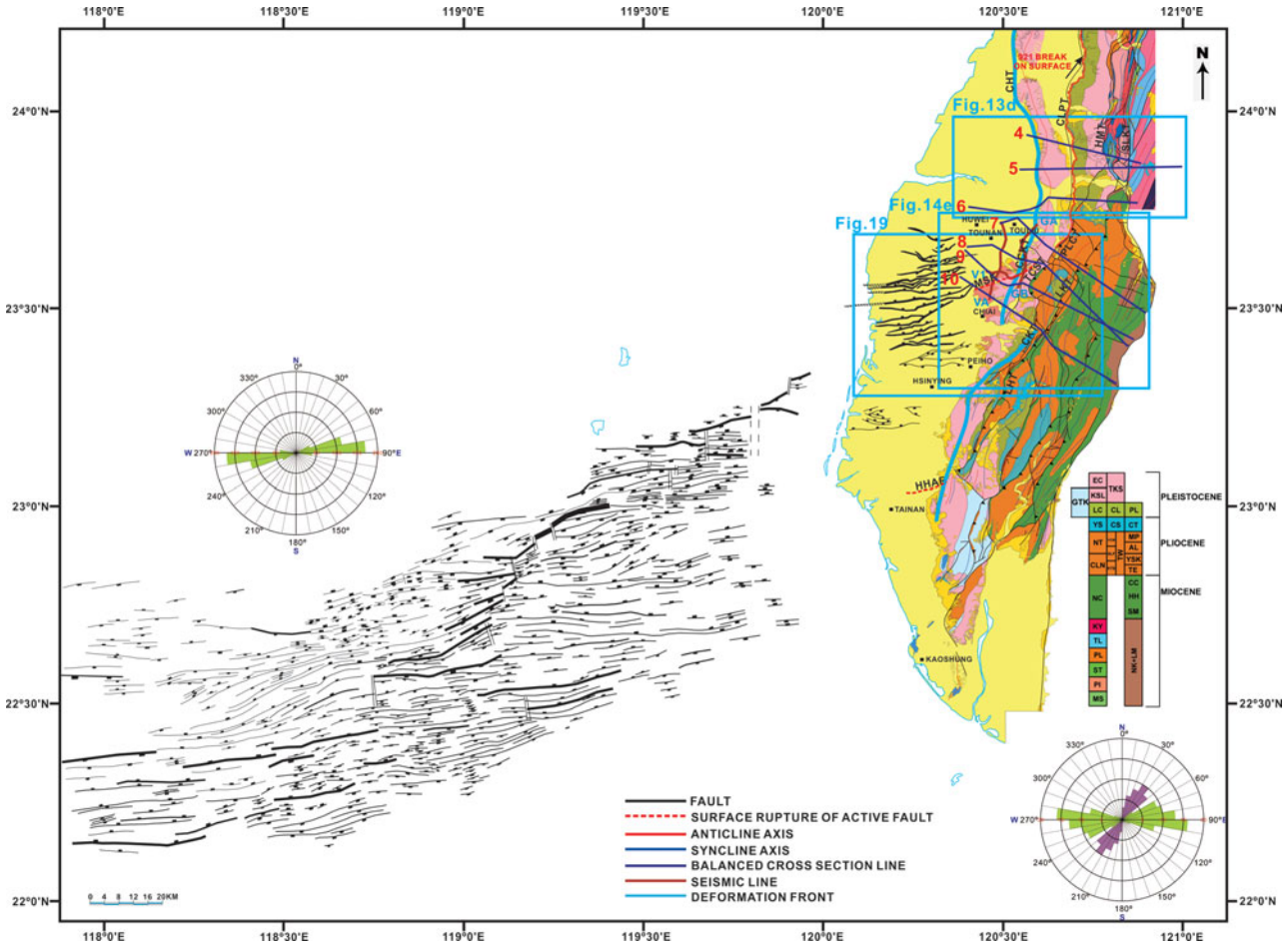

Figure 3. Tectonic map of southwestern Taiwan showing spatial distribution of various types and regional trends of all faults (compiled and modified from J. Yuan *et al*., unpub. report, 1989 and Chinese Petroleum Corporation, 1986, 1989, 1992). The rose diagrams in the upper left and lower right represent regional trends of faults in offshore and onshore areas, respectively. The locations of faults in the offshore area are from the contours of the Palaeogene top, the regional unconformity separating the Palaeogene and Neogene strata. The trends of faults in onshore area are divided into groups of that trending E–W (green) and that trending NE–SW (purple). It is noticeable that, in the offshore area and coastal plain, all the faults are normal faults. CHT – Changhua thrust; CLPT – Chelungpu thrust; HMT – Hsiaomao thrust; SLKT – Shuilikeng thrust; CCKT – Chiuchiungkeng thrust; CKT – Chukou thrust; TCST – Tachienshan thrust; PLCT – Pinlangchai thrust; LKT – Luku thrust; MTST – Matoushan thrust; MSF – Meishan fault; HHAF – Hsinhua active fault.

model of NW Taiwan. The latest review of the studies of this subject can be found in Yang *et al.* (2006). However, detailed discussion on the characteristics of this kind of structure is still rare. In Yang *et al.* (1996) the subsurface structure of the Hsinchu thrusts, which is E–W-striking and is usually regarded as having originated from normal fault reactivation, is characterized by three splays with one cutting downwards at a high angle and the others becoming soling in the lower Miocene strata (Fig. 6a). The upper Miocene and lower Pliocene sequences deposited during the latest extensional tectonics are thicker in the footwall of the high-angle thrust (Fig. 6a), indicating that the thrust was first an oppositely dipping normal fault. The structural style

https://doi.org/10.1017/S0016756816000637 Published online by Cambridge University Press

<table>
<tr><th colspan="2">Chronostratigraphy</th><th colspan="3">Lithostratigraphic units in NW and central Taiwan</th><th>Lithostratigraphic units in SW Taiwan</th></tr>
<tr><td colspan="2" rowspan="3">Pleistocene</td><td colspan="3" rowspan="3">Toukoshan Formation (TKS)</td><td>Liushuang Formation (LS)</td></tr>
<tr><td>Erhchungchi Formation (EC)</td></tr>
<tr><td>Kanhsialiao Formation (KSL)</td></tr>
<tr><td colspan="2">Cholan Formation (CL)</td><td colspan="3">Liuchungchi Formation (LC)</td></tr>
<tr><td colspan="2" rowspan="2">Pliocene</td><td colspan="3">Chinshui Shale (CS)</td><td>Yunshuichi Formation (YS)</td></tr>
<tr><td>Upper</td><td rowspan="3">Kueichulin Formation (KC)</td><td colspan="2">Yutengping Sandstone (YTP)</td><td rowspan="3">Niaotsui Formation (NT) (Tawo Siltstone, TW)</td></tr>
<tr><td>Lower</td><td colspan="2">Shiliufen Shale (SLF)</td></tr>
<tr><td rowspan="5">Miocene</td><td>Upper</td><td colspan="2">Kuantaoshan Sandstone (KTS)</td><td>Tangenshan Sandstone (TE)</td></tr>
<tr><td rowspan="2">Middle</td><td rowspan="2">Nanchuan Formation (NC)</td><td colspan="2">Shangfuchi Sandstone (SF)</td><td rowspan="2">Changchihkeng Formation (CCK)</td></tr>
<tr><td>Tungkeng Formation (TU)</td><td rowspan="2">Hopai Formation (HP)</td></tr>
<tr><td rowspan="2">Lower</td><td rowspan="3">Nankang Formation (NK)</td><td>Kuanyinshan Sandstone (KY)</td><td rowspan="3">Nankang Formation (NK)</td></tr>
<tr><td colspan="3">Talu Shale (TL)</td></tr>
<tr><td colspan="2">Peiliao Formation (PL)</td></tr>
<tr><td colspan="3">Shihti Formation (ST) (Chuhuangkeng Formation, CHK)</td><td rowspan="3"></td></tr>
<tr><td colspan="3">Taliao Formation (TK)</td></tr>
<tr><td colspan="3">Mushan Formation (MS)</td></tr>
<tr><td>Oligocene</td><td>Upper</td><td colspan="3">Wuchihshan Formation (WS)</td></tr>
</table>

Figure 4. Lithostratigraphic units of western Taiwan.

can be compared with that in the offshore area (Figs 5c, 6). Since the soled-out splays cut through the forelimb of the anticline in the hanging wall of the high-angle thrust, it is obvious that they started to develop after the high-angle normal fault was reactivated. This interpretation suggests that, without any late-coming low-angle or high-angle thrusting, the normal fault could be rotated and reactivated simply by regional contractional tectonics.

3.b. Interaction between reactivated normal faults and low-angle thrusts

Since the trend of pre-existing normal faults is oblique to the structural grain of the orogenic belt in western Taiwan, the late development of structural features affected by the inherited structures would be more complex than in any other orogenic belt. There are two aspects regarding the complexity of structural evolution in the Western Foothills of Taiwan: how the single low-angle thrusts in the fold-and-thrust belt of Western Foothills evolved and linked with the adjacent thrusts; and how they propagated towards the foreland. What will be addressed in the following is the effect of a pre-existing normal fault on the development of low-angle major thrusts.

3.b.1. Segmentation of major thrusts in the outer fold-and-thrust belt

Segmentation of the NNE–SSW-trending major thrusts by high-angle reactivated normal faults in the outer fold-and-thrust belt of onshore northwestern Taiwan (Fig. 2) has been described and analysed by Yang *et al.* (1996, 1997). Their studies show that, taking the Luchukeng thrust-Touhuangping fault-Hsincheng thrust for example, the structural features of low-angle thrusts are not symmetrical on both sides of the high-angle transverse fault. In the geological map (Fig. 2), the southern part of the low-angle Luchukeng thrust and the accompanied fold are cut through, not terminated, by two E–W-trending transverse faults: the Lungkang fault and the other transverse fault to its south. The northern end of the thrust is cut off by another transverse fault, the Touhuanping fault, and separated from the low-angle Hsincheng thrust to the north. While the sense of offset between the Hsincheng and Luchukeng thrusts is sinistral across the Touhuanping fault, the southwestern segments of the Luchukeng thrust are offset by the Lungkang and the second transverse faults in a dextral sense. An interpreted seismic section striking parallel to the low-angle thrust (Fig. 7) demonstrates that, on the southern side of the transverse fault, the low-angle Luchukeng thrust cuts up-section through a

https://doi.org/10.1017/S0016756816000637 Published online by Cambridge University Press

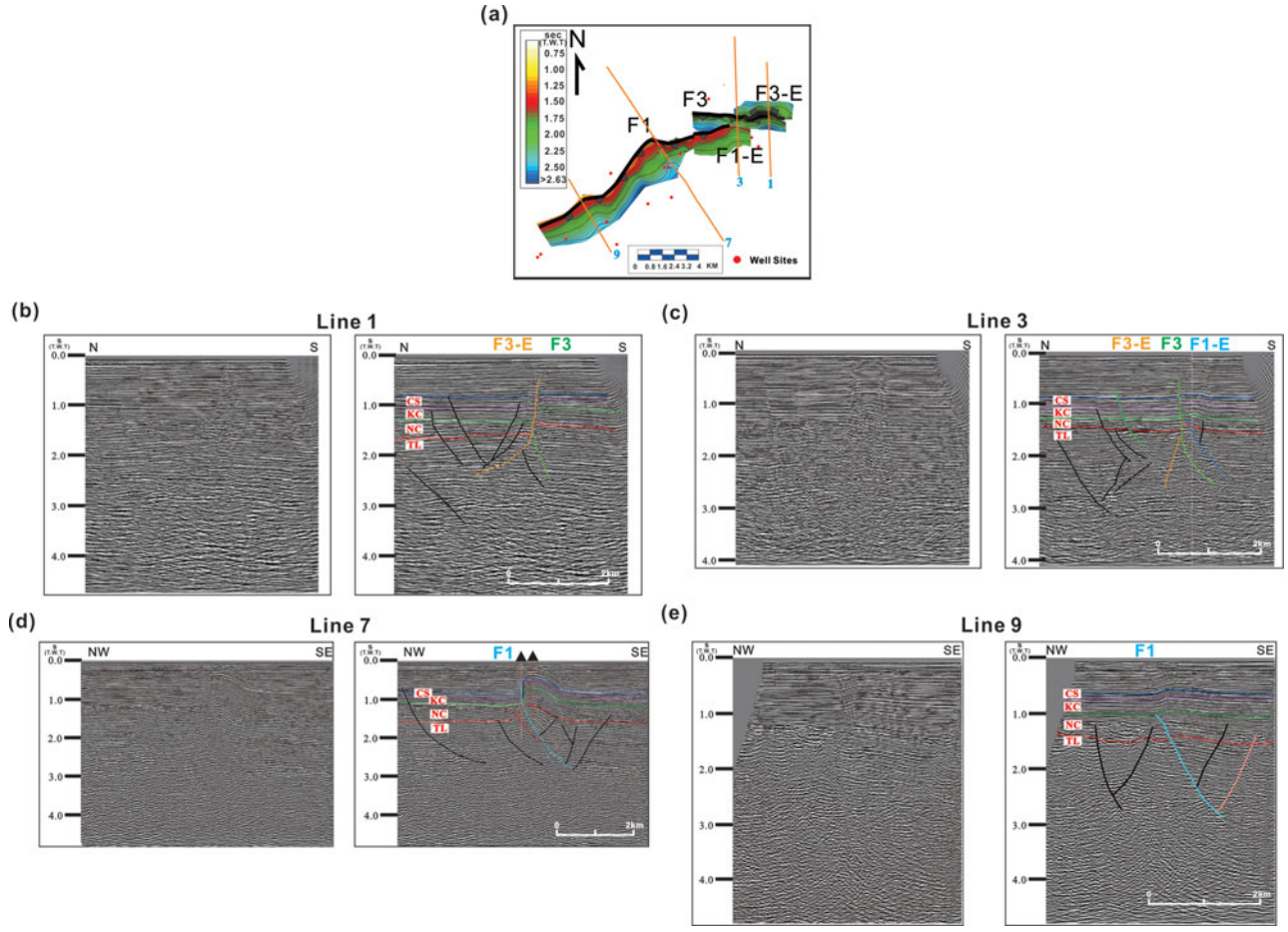

Figure 5. Reactivation of single normal faults in offshore northwestern Taiwan. (a) Geometry of fault plane and the lateral variation in fault type and dip direction of reactivated normal fault array. See the location of map in Figure 2. (b–e) A series of seismic sections, showing how displacement of reactivation increases laterally from the eastern part of a reactivated normal fault (F3) to its western part and is transferred to the next reactivated normal fault (F1). Section lines 1 and 3 show that F3-E has been rotated by reactivation displacement along F3 and its shallow part merges with F3. See ages of the formations in Figures 2 and 4.

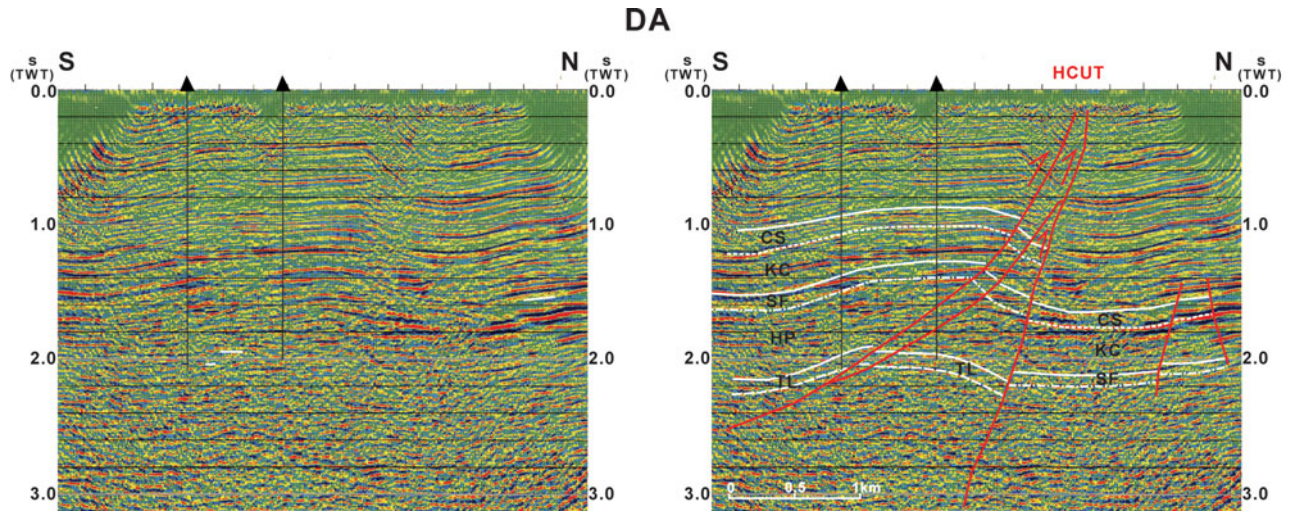

Figure 6. Seismic section in outer fold and thrust of northwestern Taiwan showing splays of high-angle reactivated normal faults. Line DA shows three splays of the Hsinchu fault in the subsurface (modified from Yang *et al.* 1996). The splays that are soled-out in the lower Miocene strata are constrained by well-bore data and the high-angle splay is interpreted using the cut-off strong reflectors in the footwall of the splays. The splays cut through the forelimb of the anticline in the hanging wall of the high-angle Hsinchu fault. See locations of the seismic sections and ages of the formations in Figure 2.

https://doi.org/10.1017/S0016756816000637 Published online by Cambridge University Press

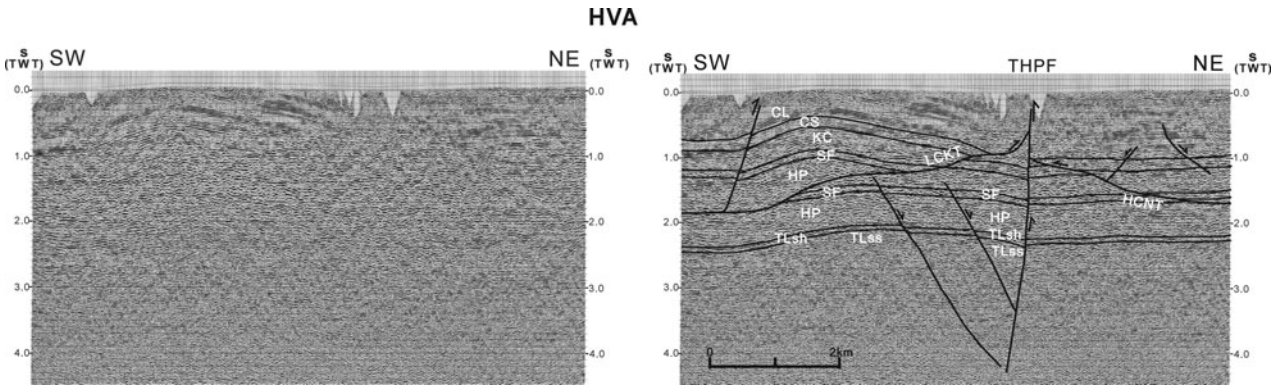

Figure 7. Seismic sections demonstrating interaction between the NNE-SSW trending major thrusts and high-angle reactivated normal faults in the fold-and-thrust belt of onshore northwestern Taiwan (Yang *et al.* 2006). See locations of seismic sections in Figure 2. Seismic section is running across a transverse fault, the Touhuanping fault, in the outer fold-and-thrust and demonstrating different structural features on both sides of the fault. On the southwestern side of the transverse fault, a thrust fault, the Luchukeng thrust, is merged with the shallow part of the high-angle fault and forms its own lateral ramp while another thrust, the Hsincheng thrust, on the northeastern side of the high-angle fault is cut off by the fault. See locations of the seismic sections and ages of the formations in Figure 2.

lateral ramp to meet the transverse fault, whereas on the other side the low-angle Hsincheng thrust was sharply cut off by the transverse fault (Yang *et al.* 1997, 2006).

The subsurface structure of the Luchukeng thrust is reconstructed in detail using a grid of interpreted seismic sections across the structure. The Yunghoshan anticline is cut through by the low-angle Luchukeng thrust, which is folded conformably with the anticline in the subsurface (Fig. 8a). Such a structural style is structurally different from the Chinshui structure, which is rather characterized by a simple anticline (Fig. 8b) although cut through by a high-angle thrust. The reconstructed geometry of the fault plane shows that the low-angle thrust extends southwards and changes to a high-angle thrust cutting through the forelimb of the Chinshui anticline (Fig. 9). There are two lateral ramps striking ENE–WSW at both ends of the NNE–SSW-trending low-angle thrust. The separation between the stratal cutoff lines on the hanging wall and footwall decreases gradually towards the SW and diminishes abruptly at the place where the thrust is cut through by the Lungkang fault.

3.b.2. Development of major thrust geometry in inner fold-and-thrust belt

In the southern part of onshore northwestern Taiwan, the San-I thrust strikes NNE–SSW on the surface, extending northwards and turning into an E–W-aligned trend at its northern end (Fig. 2). In its hanging wall adjacent to the fault trace, the stratal boundaries are running almost parallel to the bending fault trace. The bend of fault trace implies a 3D subsurface geometry such that the E–W-trending fault segment reflects the lateral ramp of the low-angle thrust (Hung & Wiltschko, 1993). In the footwall of the E–W-striking San-I thrust, the southern end of the steeply dipping western limb of the Chuhuangkeng anticline is cut off by the thrust. In Hung & Wiltschko (1993), a balanced cross-section across the northernmost part of the hanging wall of the thrust shows that the cut-off Chuhuangkeng anticline on the surface actually extends southwards in the subsurface and becomes the structure in the footwall of the thrust, where the low-angle thrust is characterized by an upfolded geometry. The folded strata in the central part of hanging wall of the thrust are striking NE–SW (Fig. 2), implying another characteristic of subsurface 3D geometry of the thrust and footwall structure.

A series of interpreted seismic sections and published balanced cross-sections (Yang *et al.* 2007) show that the San-I thrust in the subsurface changes from convex-upwards to concave-upwards toward the SW (Figs 10a–c, 11a–c). The convex-upwards geometry is related to upfolding in its footwall, in which the localized fold structure is tighter towards the NE. The structure of the footwall of the thrust is also characterized by a series of pre-existing high-angle normal faults. The fold structure is closely accompanied by a convex-upwards high-angle fault, which coexists with a series of pre-existing high-angle normal faults (Figs 10a–c, 11a–c). A reconstructed structural contour map indicates that the convex-upwards high-angle fault is striking ENE–WSW (Figs 10d, 11d), parallel to the general trend of the reactivated normal faults to the north. The magnitude and sense of displacement are not uniform along the fault plane. The largest magnitude of original normal fault displacement along the high-angle fault appears in the northernmost part of the area, where it is characterized by the tightest fold in the footwall of the San-I thrust (Fig. 11a). The convex-upwards high-angle fault is a reactivated normal fault and its formation mechanism is similar to that of the Hsinchu fault.

In central Taiwan where the Peikang Basement High stands in front of the Western Foothills, the thickness of the upper Miocene and Pliocene strata in the hanging wall of the Chelungpu-Tachienshan-Chukou thrust is twice that in the footwall (Fig. 12; Yang *et al.* 2007). Balancing the thickening of Pliocene strata in the

https://doi.org/10.1017/S0016756816000637 Published online by Cambridge University Press

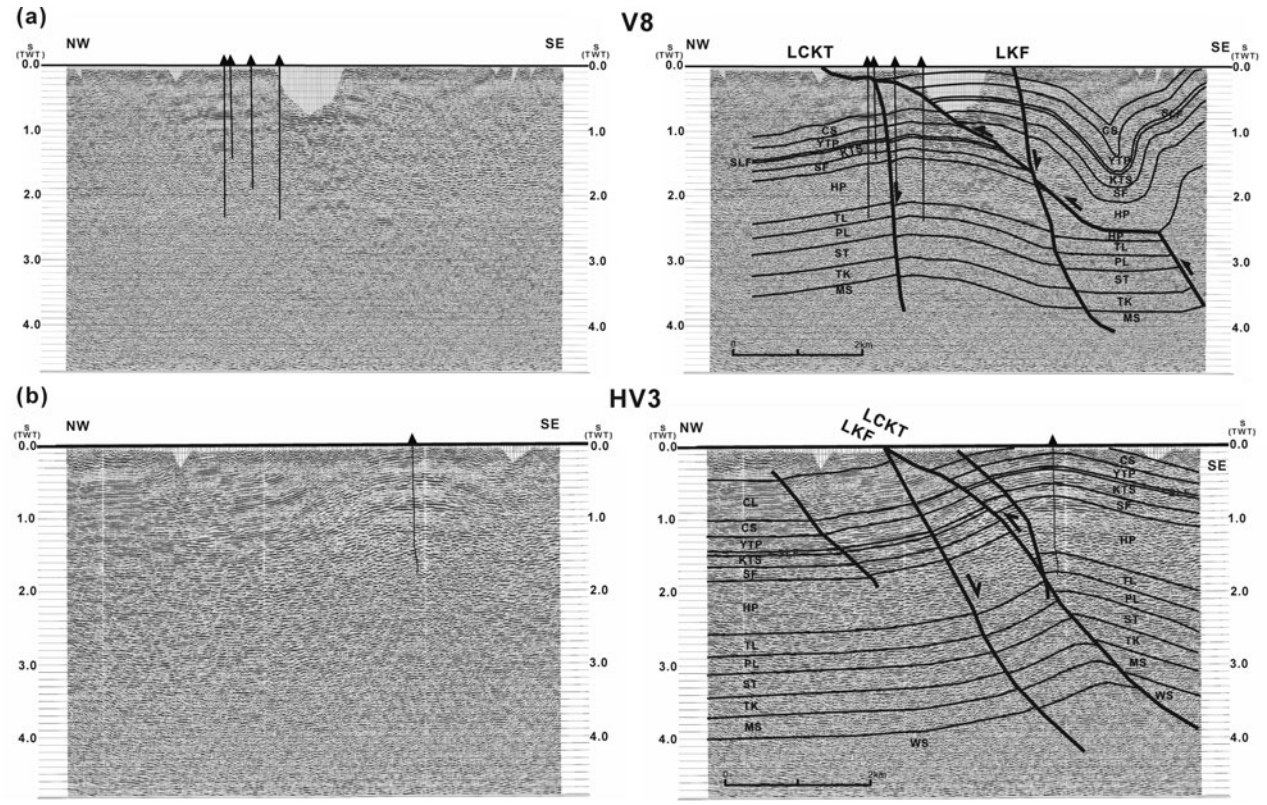

Figure 8. Seismic sections running through the Luchukeng NNE–SSW-trending thrust in the outer fold-and-thrust belt, showing variation in the structural styles in the two adjacent Yunghoshan and Chinshui structures. (a) Seismic section showing structural feature of the low-angle Luchukeng thrust, and (b) that showing structural feature of the high-angle Luchukeng thrust in the subsurface. See locations of the seismic sections and ages of the formations in Figure 2.

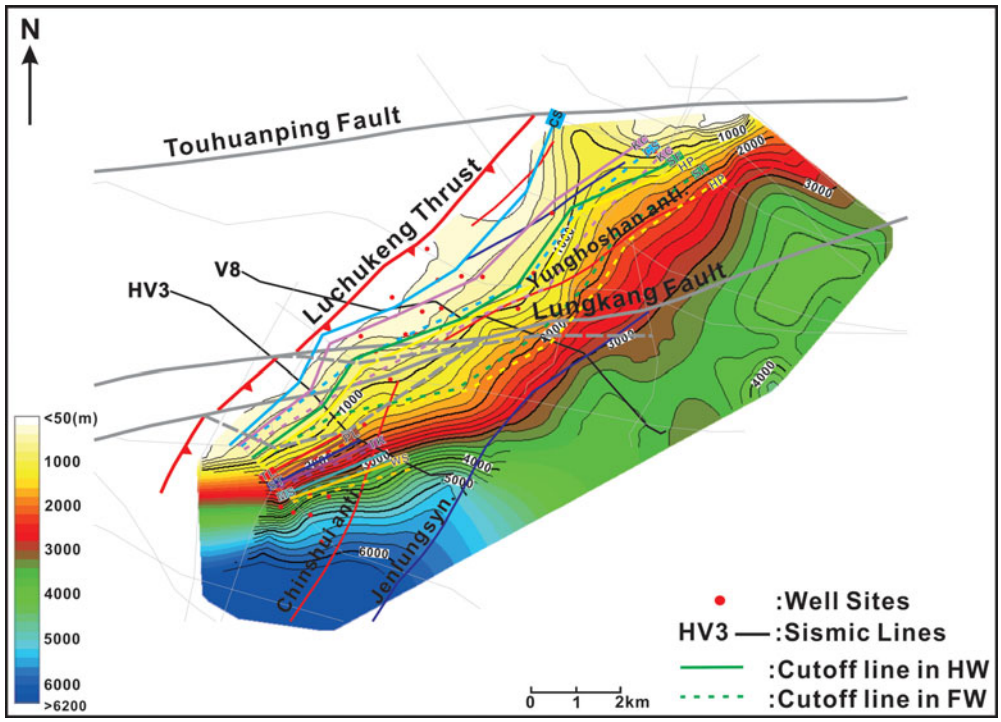

Figure 9. 3D geometry of the Luchukeng thrust in the subsurface and cutoff lines of the hanging wall and footwall strata. The thrust has two lateral ramps, which are parallel to transverse faults at both ends of the fault. It is noticeable that the southern lateral ramp, although cut through by the Lungkang fault, extends all the way down to the lower part of the Chinshui structure. See locations of the seismic sections and ages of the formations in Figure 2.

https://doi.org/10.1017/S0016756816000637 Published online by Cambridge University Press

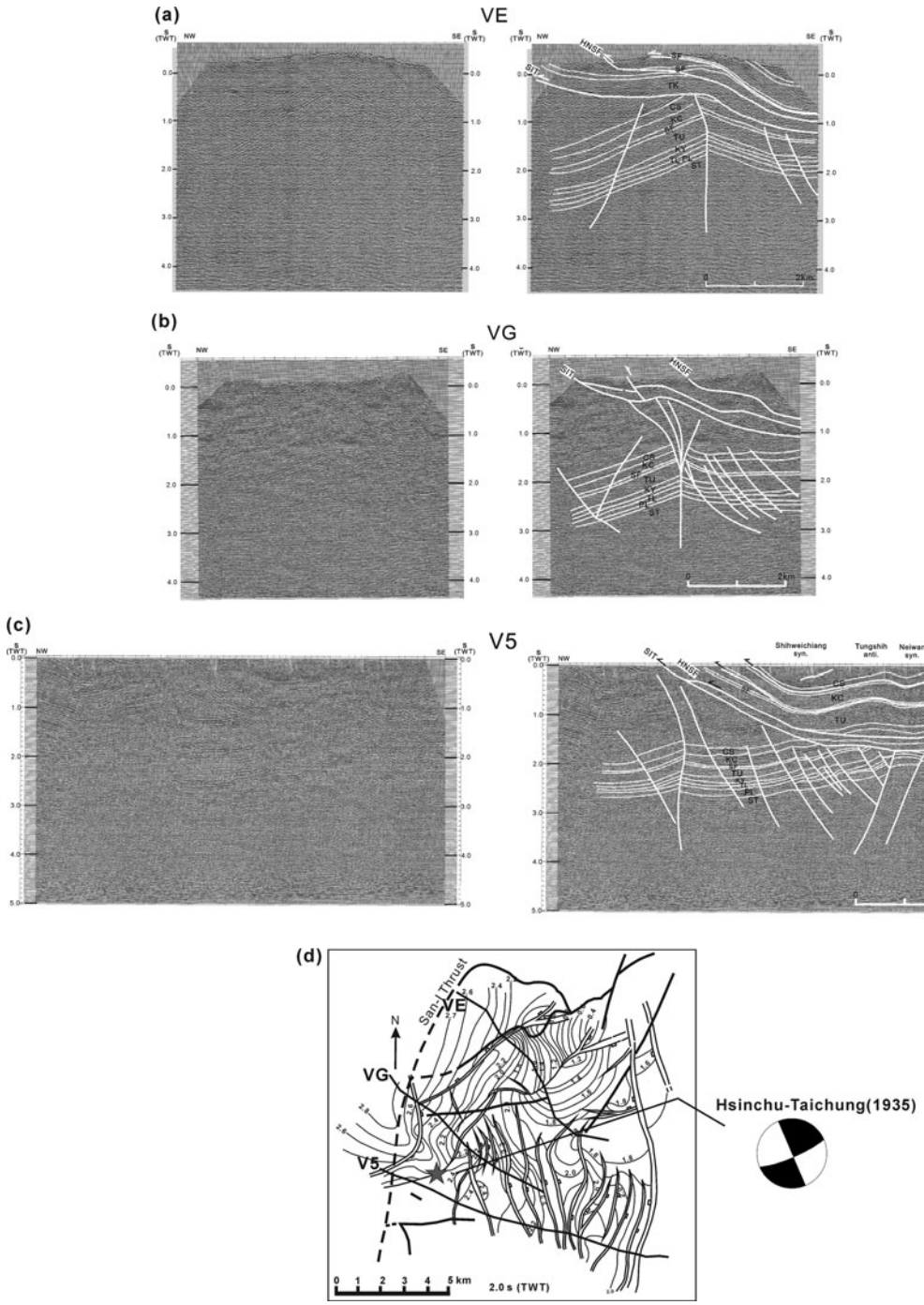

Figure 10. Variation in subsurface structural feature of the San-I thrust and its footwall constrained by seismic interpretation. (a–c) Seismic sections showing that the San-I thrust in the subsurface changes from convex-upwards to concave-upwards toward the SW. The seismic sections also show a series of non-reactivated normal faults and a reactivated high-angle normal fault in the footwall of the thrust. Interpretation of seismic section V5 is from Yang *et al.* (2007). (d) Structural contours of the Talu Formation top in the footwall of the San-I thrust showing fault structures with various trends. The contour map shows the epicentre of the Hsinchu-Taichung Earthquake (1935) at the reactivated normal fault (Lin, 2005), which is trending ENE–WSW. See locations of the seismic sections in Figure 10d and ages of the formations in Figures 2 and 4.

hanging wall of the major thrusts requires that normal faults exist somewhere to the east of the exposed major thrusts and beneath the décollement (Figs 13, 14).The subsurface geometry of the Tachienshan-Chukou thrust also varies from the north to the south, depending on the magnitude of the slip along the Chiuchiungkeng fault (Fig. 14b–d). In the northern part of the area, the greater slip along the Chiuchiungkeng fault formed the lower-angle Tachienshan thrust. To the south where displacement along the Chiuchiungkeng fault decreases to zero, the Chukou thrust fault appears as a high-angle thrust cutting up through the surface. The variations in structural features along-strike of the thrust system and the restoration of two balanced cross-sections (Figs 13–16) suggest that, during the development of the Chelungpu and Tachienshan thrusts, the foreland-ward

https://doi.org/10.1017/S0016756816000637 Published online by Cambridge University Press

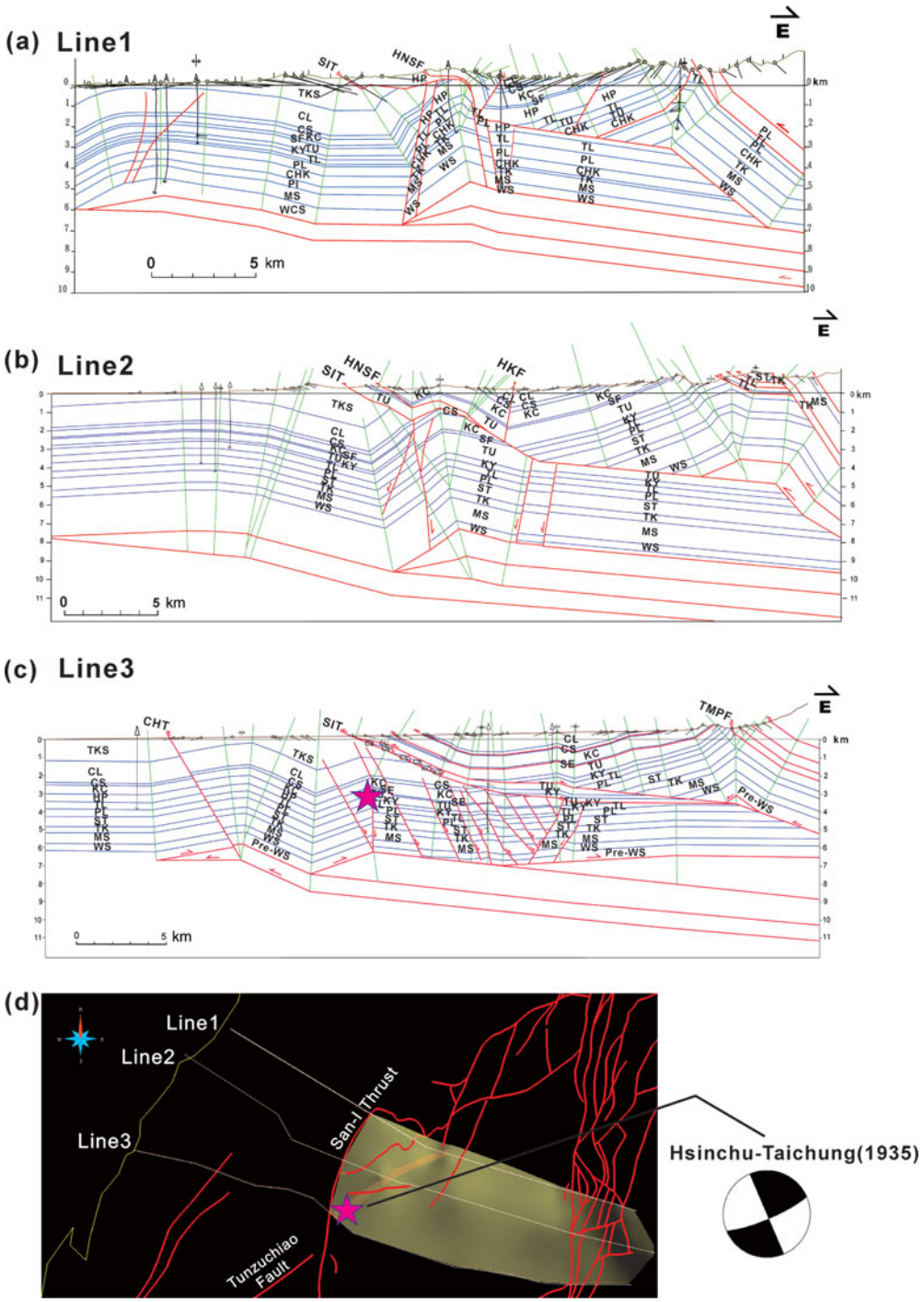

Figure 11. Balanced cross-sections and 3D geometry of faults showing variation in subsurface structural features of the San-I thrust and its footwall. (a–c) Balanced cross-sections run through the the San-I area and show variation in the geometry of upfolded San-I thrust and tightness of the fold in its footwall in the subsurface (Yang *et al.* 2007). In the balanced cross-section running through the southern part of the area San-I thrust is characterized by concave-upwards geometry, which represents the original geometry before the thrust was upfolded. The non-reactivated normal faults and the high-angle reactivated normal fault in the footwall of the thrust is interpreted based on seismic interpretation. (d) The 3D geometry of the low-angle San-I thrust and the high-angle reactivated normal fault is constructed by linking the faults on the balanced cross-sections. It is shown that, in the footwall of the low-angle San-I thrust (yellow colour), the high-angle reactivated normal faults (dark red colour) is trending ENE–WSW, parallel to that of the Tunzuchiao fault, the surface rupture of the Hsinchu-Taichung Earthquake (1935). See locations of the balanced cross-sections in Figure 2 and ages of the formations in Figures 2 and 4.

propagating décollement or low-angle thrusts met the high-angle normal faults and utilized the shallow part of the normal fault as a ramp to climb up to the surface. The ramps were then translated by slip along the Changhua and Chiuchiungkeng thrusts, and left the cut-off normal faults beneath the décollements. The localized thrust ramps and normal faults in different cross-sections can be connected to demonstrate the 3D geometry of the subsurface high-angle fault plane, indicating that their strikes are oblique to that of the major

https://doi.org/10.1017/S0016756816000637 Published online by Cambridge University Press

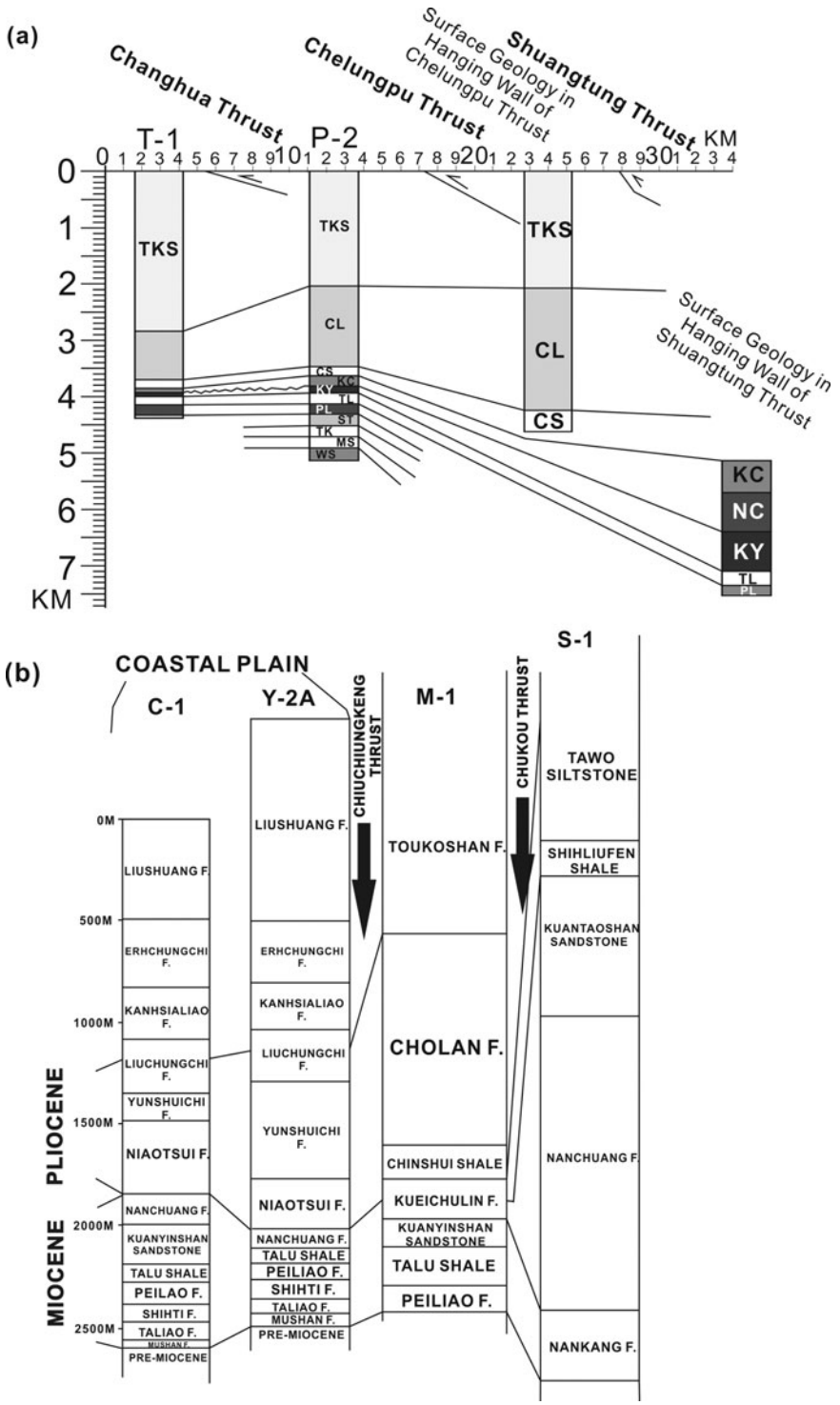

Figure 12. Stratal thickening across the major thrusts in (a) central and (b) southwestern parts of the fold-and-thrust belt (Yang *et al.* 2007). The thickened strata in the hanging wall of the major thrusts are those deposited during the latest extension and foreland basin periods. The strata on both sides of the major thrusts are given different formation names, indicating different lithofacies for the strata. This implies that either the major thrusts result from reactivation of large-scale normal faults or they are low-angle thrusts with significant horizontal component of slip. Balanced cross-sections in Figures 13 and 14 favour the latter.

thrust in Western Foothills but parallel to that of the pre-existing normal fault in the foreland basin (Figs 13d, 14e).

4. Today's active normal fault reactivation

In onshore western Taiwan, the surface traces of some thrusts that were addressed in the previous sections are still active today and have been defined as active faults by the Central Geology Survey, Taiwan (Lin *et al.* 2000). Some of them and the others located in the front of the fold-and-thrust belt are striking parallel to the structural trends of the regional extensional tectonics, and may therefore be related to normal fault reactivation. Some active faults are major thrusts that are viewed as a boundary between the outer and inner

https://doi.org/10.1017/S0016756816000637 Published online by Cambridge University Press

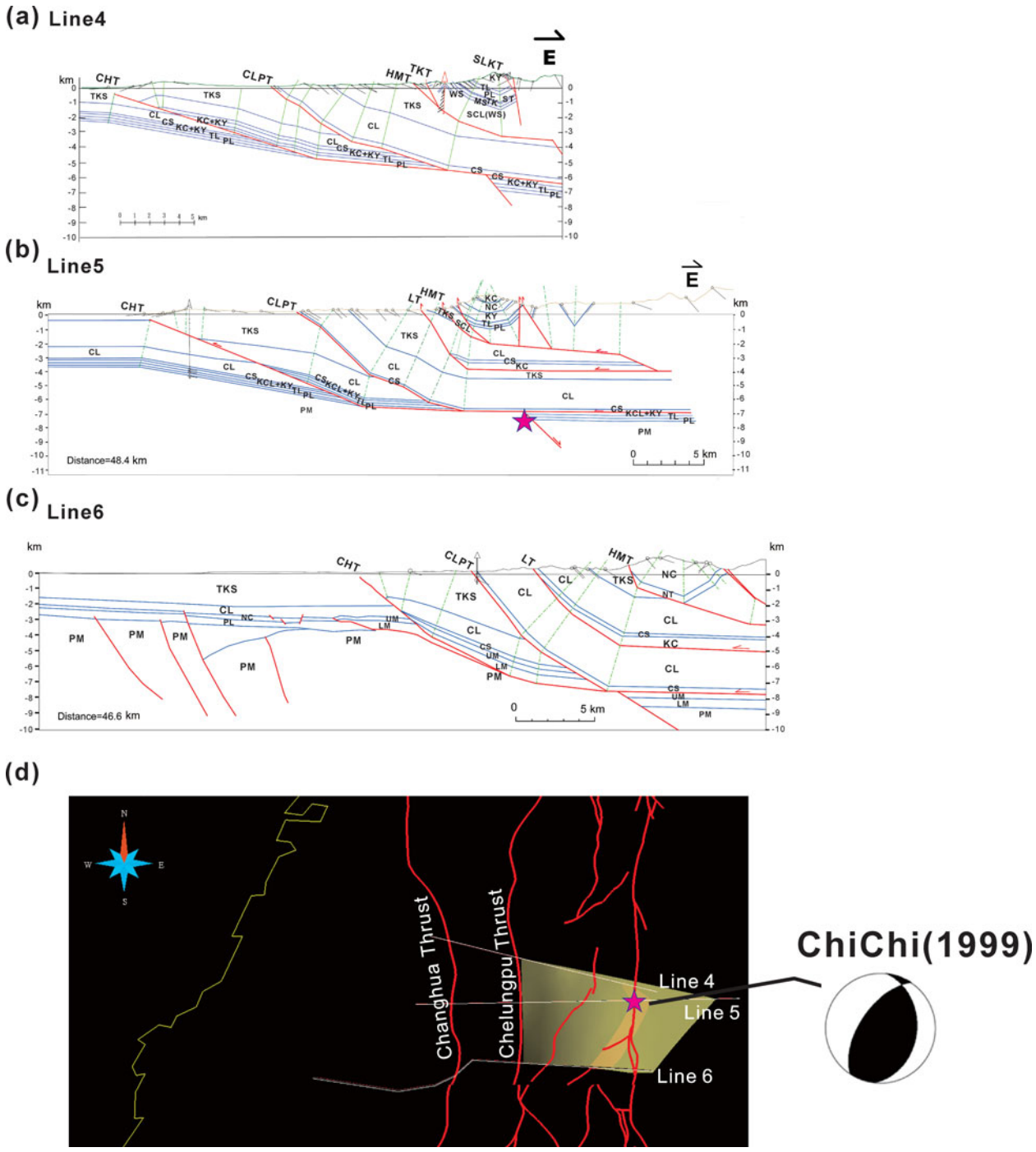

Figure 13. A series of balanced cross-sections through the fold-and-thrust belt in central Taiwan (Yang *et al.* 2007). (a) On line 4, the décollements of the Changhua and Chelungpu thrusts are along different formations but merged with each other in the subsurface. A normal fault exists underneath the common décollement and accommodates the thickened Cholan Formation in the hanging wall of the Chelungpu thrust. (b) The star on line 5 represents the main shock of the Chi-Chi Earthquake and is located very close to the pre-existing normal fault underneath the common décollement. (c) The structural features on line 6 are very similar to that on lines 4 and 5, but the normal fault underneath the décollement is located closer to the bend from the décollement to the ramp of the Chelungpu thrust. (d) The 3D geometry of the low-angle Chelungpu thrust and the high-angle reactivated normal fault is constructed by linking the faults on the balanced cross-sections and shows that, in the footwall of the low-angle Chelungpu (yellow colour), the high-angle reactivated normal faults (dark red colour) is trending ENE–WSW. See locations of the balanced cross-sections in Figure 3.

fold-and-thrust fault (Fig. 3). Some historical earthquakes that have been connected to the surface rupture of such an active fault could be related to high-angle normal faults that have been involved in low-angle thrusting. In this section, we attempt to identify the normal fault reactivation in today's active tectonics via a group of earthquakes with similar properties to that of fault plane solutions and subsurface structural features of coseismic surface ruptures. Earthquakes used in this paper were relocated using a previously published 3D velocity model (Rau & Wu, 1995). The average uncertainties of earthquake

https://doi.org/10.1017/S0016756816000637 Published online by Cambridge University Press

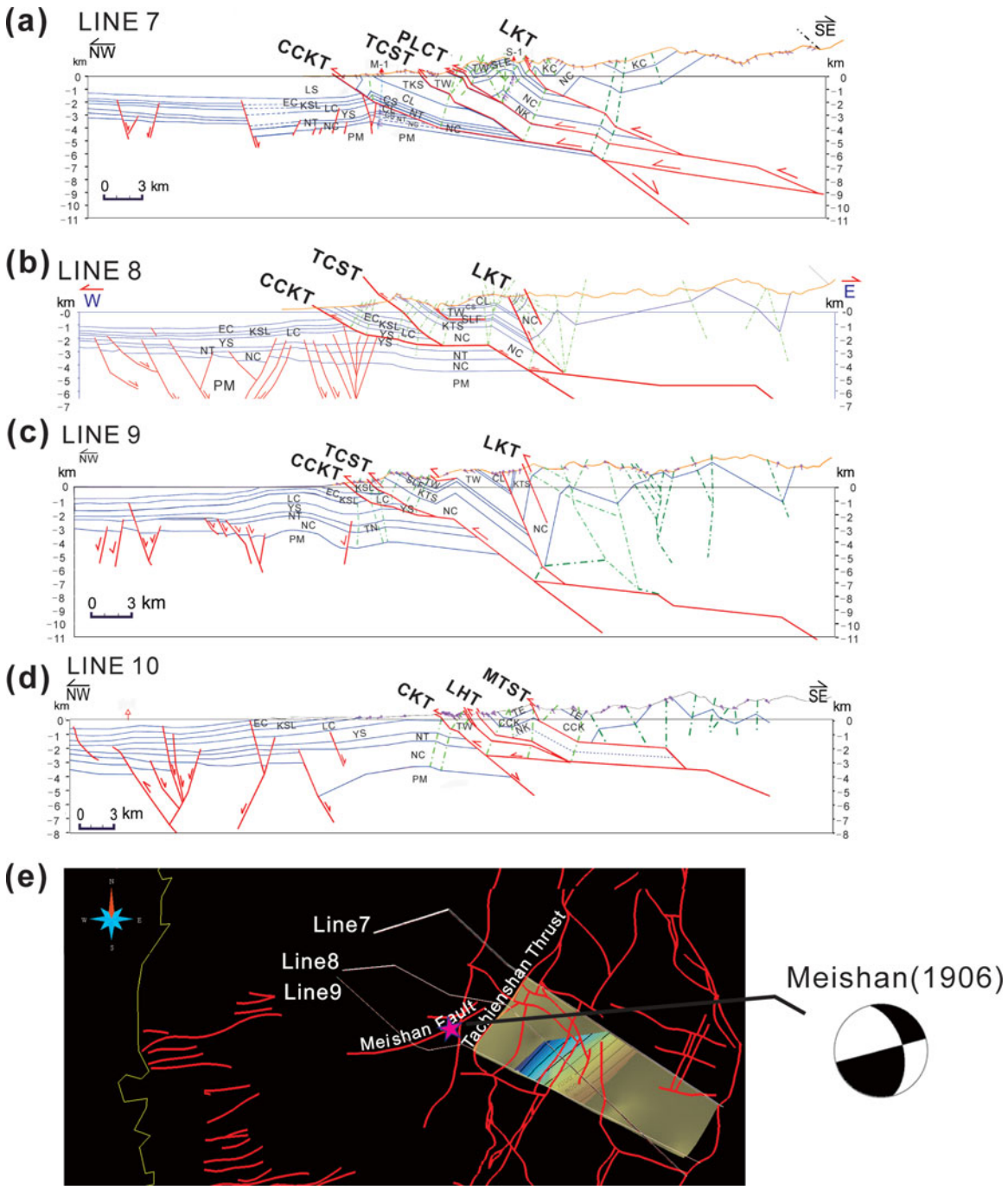

Figure 14. (a–d) A series of balanced cross-sections through the foreland basin and fold-and-thrust belt in southwestern Taiwan. Also shown in the figure is (e) the 3D geometry of the Tachienshan thrust (yellow colour) and a normal fault (blue colour with contours) that acts as the frontal ramp of the thrust in the subsurface. Lines 7, 8 and 10 are from Yang *et al.* (2006, 2007). The contours of the normal fault underneath the Tachienshan thrust indicate that the strike of the normal fault is parallel to that of the Meishan fault.

locations relocated by the 3D model are estimated to be 3 km horizontally and 5 km vertically. By comparing with a few recent tomographic studies of Taiwan (e.g. Wu *et al*. 2007) using more recent data, the main features of the model do not differ much in comparison with those of Rau & Wu (1995). For the earthquake focal mechanisms with $M_L \geq 3.0$ which occurred prior to June 2006, we used the focal mechanism database determined by the approach incorporating first motions and *SH*/*P* amplitude ratios (Rau, Wu & Shin, 1996). For the events that occurred between June 2006 and December 2014, we used either the centroid moment tensor (CMT) or the first-motion solutions determined by the Central Weather Bureau for earthquakes with $M_L > 3.5$. For the fault plane solutions of the main shock of the earthquake which occurred early last century, we refer to the studies of Sheu, Kosuga & Sato (1982), Cheng (1995) and Lin *et al.* (2013).

https://doi.org/10.1017/S0016756816000637 Published online by Cambridge University Press

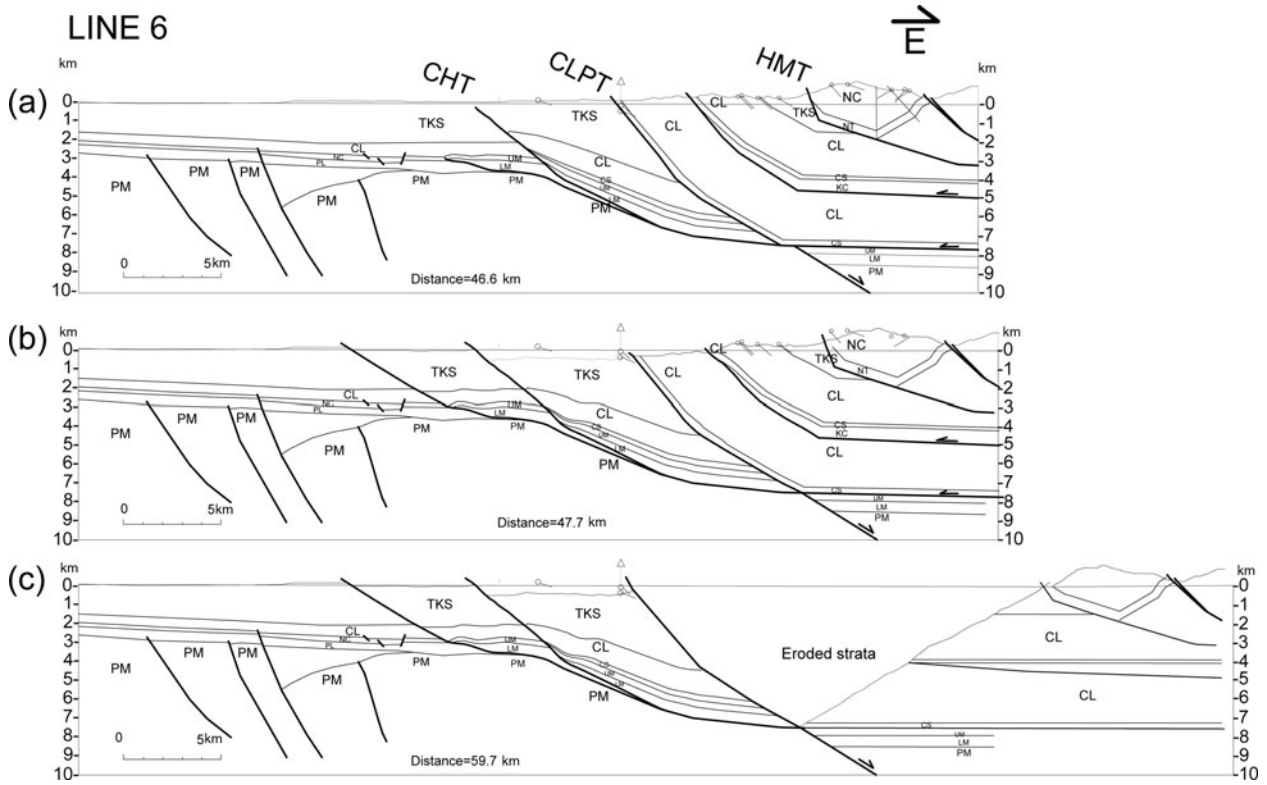

Figure 15. Restoration of line 6 showing evolution of slip along the Chelungpu and Changhua thrusts. (a) Balanced cross-section of line 6. (b–c) Restorations made on the slip along the Changhua thrust and then the Chelungpu thrust. The restoration also demonstrates how the locations of the normal faults underneath the décollement in all the balanced cross-sections are determined by restoring the slip along the Changhua thrust to make the ramp of the Chelungpu thrust on the line of the normal fault.

4.a. Active normal fault reactivation in NW Taiwan

The hypocentre of the main shock of the Hsinchu-Taichung Earthquake which occurred in 1935 has been relocated by Sheu, Kosuga & Sato (1982), Cheng (1995) and Lin *et al.* (2013) and is very close to the reactivated normal fault beneath low-angle San-I thrust in northwestern Taiwan (Lin, 2005). The trend of the Tuntzuchiao fault, a surface rupture of the earthquake, is consistent with the strike of the reactivated normal fault beneath the low-angle thrust (Figs 2, 10d, 11d). A series of earthquake epicentres in that area that are characterized by strike-slip component are mainly located along a belt that is also parallel to the main reactivated normal faults in the footwall of the San-I thrust (Figs 2, 17). The close relationship among the seismicity, historical earthquake and the reactivated normal fault indicate that normal fault reactivation in the footwall of the San-I thrust, although not exposed, remains ongoing.

4.b. Active normal fault reactivation in SW Taiwan

The epicentre of the main shock of the Meishan fault which occurred in 1906 has been relocated on the fault in the subsurface of southwestern Taiwan (Fig. 3; Cheng, 1995). The surface rupture is characterized by thrusting its southern side over the northern side, with dextral strike-slip component (Lin *et al.* 2000). A subsurface structural feature of the Meishan fault can be depicted with interpretation of seismic profiles running through the fault and the frontal thrust (Fig. 3). Interpreted seismic sections across the Meishan fault show a typical positive flower structure for the fault, indicating that the surface rupture is one of the splays in the subsurface (Fig. 18a, b). The positive flower structure implies deformation with contractional component across the fault. However, all the splays, except one or two that are characterized by overthrusting on its southern side and may represent the main active fault on the surface, are normal faults. In map view, the Meishan fault can be extended southwestwards to link a non-reactivated normal fault with downthrow on its northern side (Fig. 3). The high-angle fault feature occurs not only in the front of the fold-and-thrust belt but also in the footwall of the frontal thrust (Fig. 18c). All the subsurface structural features of the Meishan fault indicate that the fault originated from a reactivated normal fault that has been partly thrust by the frontal thrust. In addition, the fault plane solutions for today's earthquakes indicate that those with strike-slip component are highly related to the deformation along the main reactivated normal fault (Fig. 19).

4.c. Active normal fault reactivation in the inner fold-and-thrust belt

In central Taiwan the 1999 Chi-Chi Earthquake caused a surface rupture of more than 80 km in length, which is

https://doi.org/10.1017/S0016756816000637 Published online by Cambridge University Press

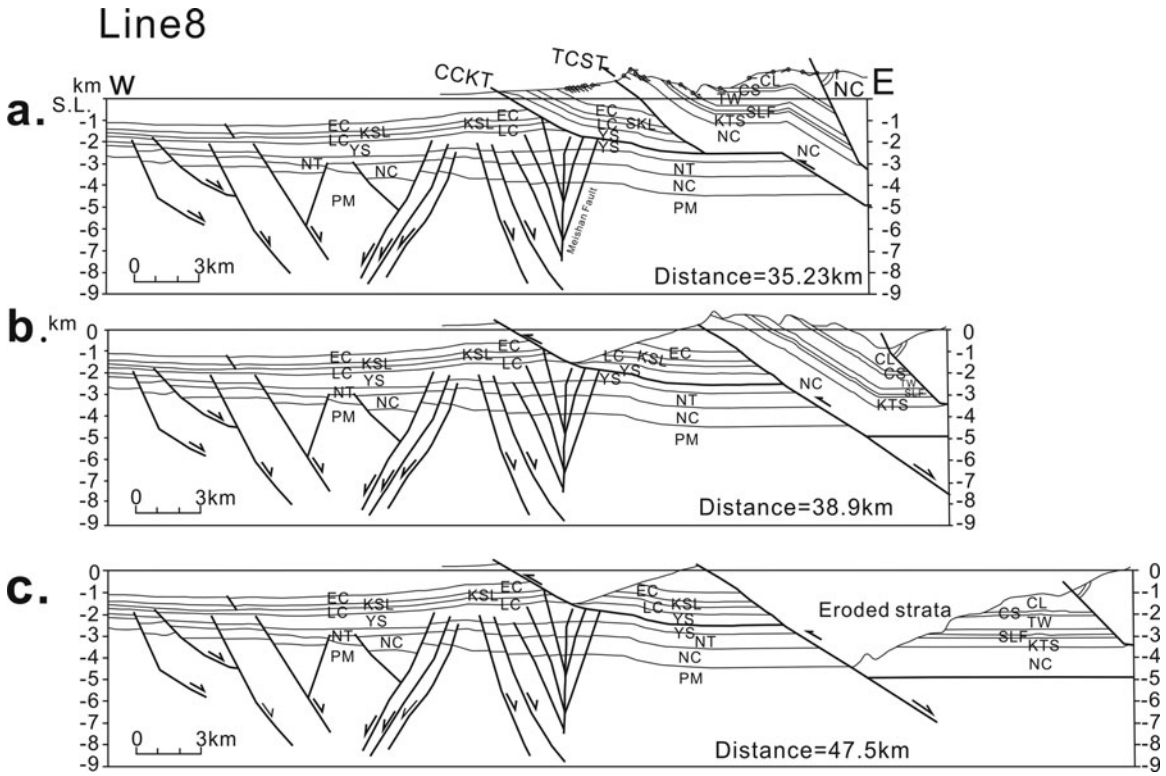

Figure 16. (a) Restoration along the thrusts on the balanced cross-section line 8. (b) Restoration is made first on the slip along the Chiuchiungkeng thrust to locate the shallow ramp of the Tachienshan thrust on the line of the normal fault. (c) At the next stage, slip along the Tachienshan thrust is restored to eliminate the fault-bend structure in the hanging wall of the thrust. The geometry of the Tachienshan thrust fault in (b) can be compared to that of the Chukou thrust on line 10.

almost identical to the exposed Chelungpu thrust. However, a connection between the Chi-Chi Earthquake and the subsurface structure of the Chelungpu thrust is still under debate (Mouthereau, Angelier & Lee, 2001; Hung & Suppe, 2002; Wang *et al.* 2002; Yue, Suppe & Hung, 2005; Yang *et al.* 2007). The fault plane solution for the main shock indicates that the dip angle of the slip surface is around 30° and that the hypocentre is at a depth of 8 km below sea level (Fig. 13b). Both dip angle and depth of the main shock are not consistent with those of the décollement of the Chelungpu thrust, but very close to the normal fault beneath the décollement (Fig. 13b; Yang *et al.* 2007). This suggests that the basement-involved normal fault plane could still play an important role in triggering disastrous earthquakes. Analysis of the recent (2013) M_L 6.2 and M_L 6.5 Nantou Earthquakes (Chuang *et al*. 2013) seems to justify such a viewpoint.

In some cases, the location of the hypocentres of some major earthquakes in the frontal part of the Western Foothills in southwestern Taiwan strongly suggest that normal faults used as high-angle ramps for the major thrusts could have triggered these earthquakes. The situation appears in southwestern Taiwan, where several earthquakes have been located very close to the normal fault plane where the shallow part has been utilized as the ramp of the Tachienshan thrust (Yang, 2007; Huang, 2009).

5. Discussion

5.a. Development of reactivated basement-involved normal faults

Comparing with that in offshore southwestern Taiwan (Fig. 3), the high-angle faults in offshore northwestern Taiwan (Fig. 2) are longer and continuously extend into the onshore. Linkage of shorter normal faults into longer faults through normal fault reactivation must have played an important role. The inversion structures in northwestern Taiwan show several important characteristics of normal fault reactivation occurring in the frontal part of the fold-and-thrust belt. First, some examples of high-angle normal faults reactivated by low-angle thrusting with opposite dipping direction have been documented in some orogenic belts (Welbon & Butler, 1992; Butler, Tavarnelli & Grasso, 2006). What we have observed in offshore northwestern Taiwan is the case of a normal fault reactivated by another high-angle reactivated normal fault (Fig. 5a–c). Second, in the situation of oblique inversion such as northwestern Taiwan, reactivation could happen in any segments of the fault instead of always from the hinterlandwards end of the fault. Third, the transfer of inversion displacement between two adjacent faults could happen, very similar to that in the fold-and-thrust belt. It is also noticeable that the apparently 'curved' reactivated normal fault (F1 in Fig. 5a) is in fact composed of two

https://doi.org/10.1017/S0016756816000637 Published online by Cambridge University Press

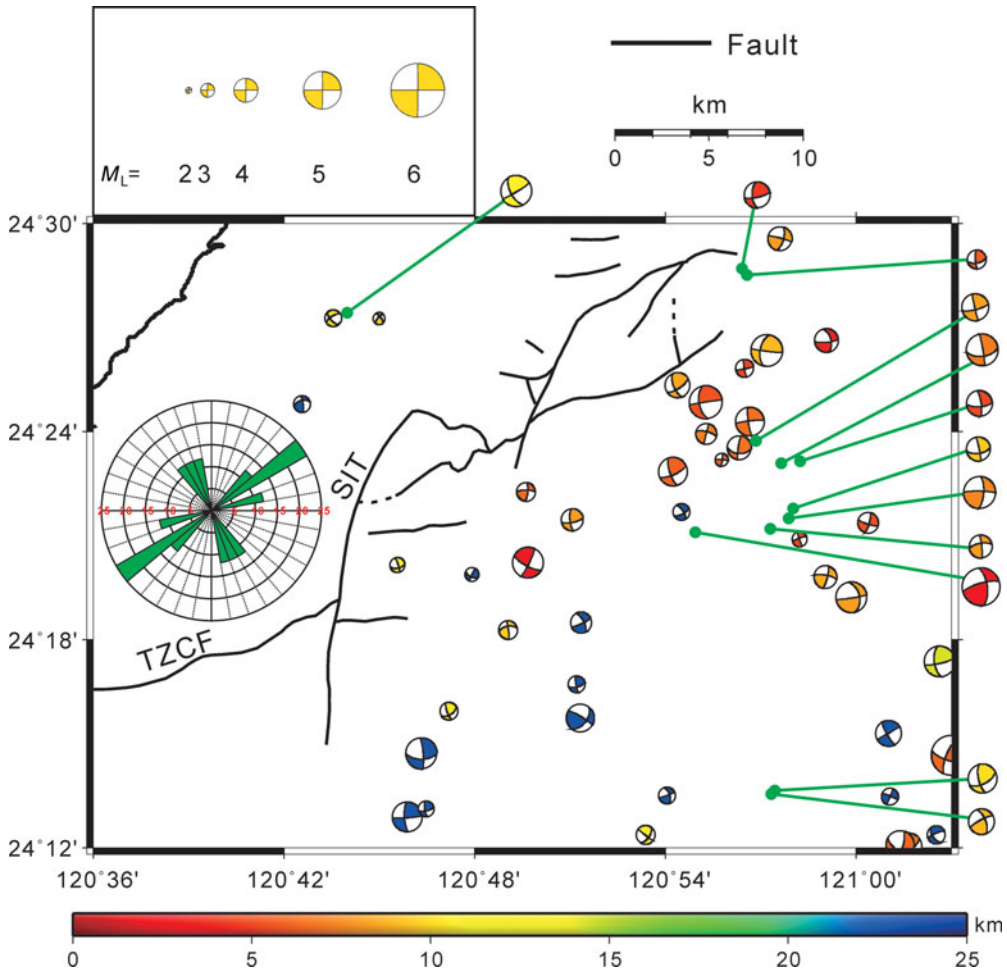

Figure 17. Distribution of strike-slip fault plane solutions in onshore northwestern Taiwan and a rose diagram showing the main trend of the fault planes in the San-I area. One set of the fault planes is trending ENE–WSW, parallel to that of the Tuntzuchiao fault.

segments with different trends. The large-scale symmetrical anticline and the corresponding largest inversion displacement also occur right at the location of the largest fault plane curvature. We propose that the two segments of the reactivated normal faults were originally two softly linked normal faults separated by a relay between the faults, and that normal fault reactivation during contractional tectonics caused the linkage of the separated normal faults and made the relay the place of the largest thrust offset along the high-angle fault (Fig. 5). The reactivated normal faults with large lateral length in the foreland basin (Fig. 2) could therefore have been formed by linkage of separated pre-existing normal faults through normal fault reactivation. Similar evolutionary models have been documented by regional geological studies (Sinclair, 1995; Carrera & Muñoz, 2013) or by physical modelling (Eisenstad & Withjack, 1995; Keller & McClay, 1995; Amilibia *et al.* 2005).

The tectonic map of northwestern Taiwan (Fig. 2) also shows that, in general, non-reactivated normal faults, reactivated normal faults and low-angle thrusts were spatially distributed in an order from west to east. To the east, the reactivated normal faults terminate at the front of boundary thrust between the outer and inner fold-and-thrust belts on the surface. The high-angle reactivated normal fault can be observed in the footwall of the low-angle Peipu-Chutung thrust in the inner fold-and-thrust belt (Yang *et al.* 1997, 2006).

In the outer fold-and-thrust belt, the strike of the subsurface Luchukeng thrust changes right across the Lungkang and the second transverse faults, parallel to that of the Lungkang fault (Fig. 9). Such structural geometry indicates two important characteristics about the interaction between the reactivated normal fault and low-angle thrust. First, during the development of a lateral propagating low-angle thrust, a pre-existing reactivated normal fault causes abrupt changes in both geometry and displacement of the thrust. Second, the Lungkang fault and the second transverse fault can apparently be viewed as tear faults to the Luchukeng thrust; this situation is however not the same as what happens on both sides of the Touhuanping fault to the north, where the Hsincheng and Luchukeng thrust are independent structures (Yang *et al.* 1997). Rather, it is cut through by and runs across the confining high-angle transverse faults in the subsurface. To the south, the high-angle ramp cutting through the base of Chinshui anticline should be regarded as the southwards extensional part of the low-angle Luchukeng thrust. The high-angle transverse faults might extend into the inner fold-and-thrust belt and become tear faults trending ENE–WSW. Such structures appear in some places

https://doi.org/10.1017/S0016756816000637 Published online by Cambridge University Press

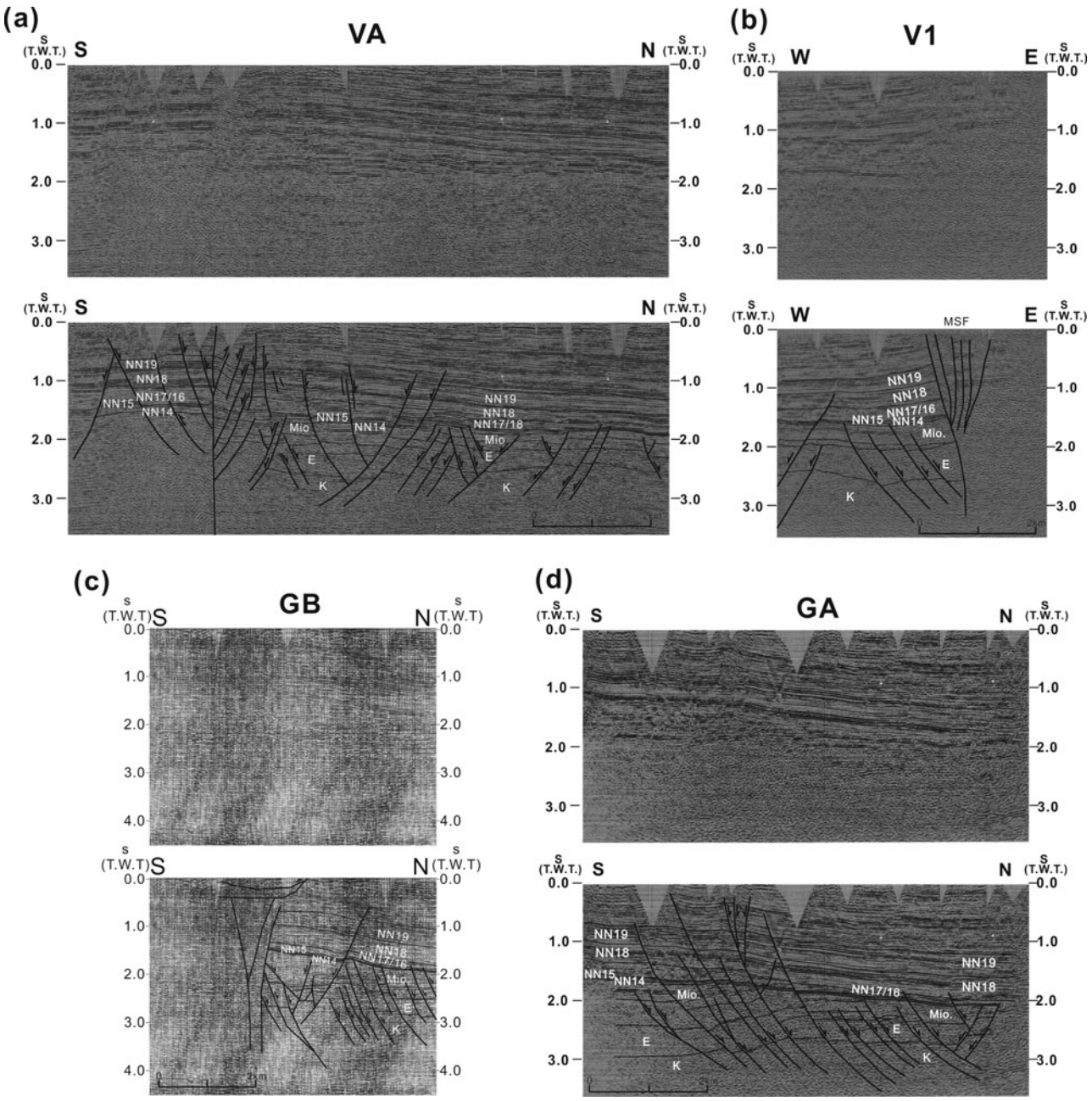

Figure 18. Interpreted seismic sections presented as constraints to depict the subsurface structure and the strike of the Meishan fault and accompanied structural style. (a) Seismic sections VA and (b) V1 show the flower structure of the Meishan fault in the subsurface of the foreland basin, indicating strike-slip component along the fault. (c) Seismic section GB reveals the Meishan fault in the footwall of the Chiuchiungkeng thrust. (d) Seismic section GA is running through a set of N-dipping normal faults and shows rising Neogene strata southwards to the Meishan fault. Similar monoclonal structure also appears in seismic sections V1 and GB. See locations of the seismic sections in Figure 3.

in the inner fold-and-thrust belt and can be manifested by a series of tear faults trending ENE–WSW in the inner fold-and-thrust belt (Fig. 2).

In onshore southwestern Taiwan, where there is a lack of reactivated normal fault in the foreland basin (Fig. 3), pre-existing normal faults have been involved in the inner fold-and-thrust belt as ramps of the major thrusts (Figs 13, 14). In this part of the Western Foothills, tear faults are mostly striking WNW–ESE to NW–SE, representing the orientation of thrust sheet translation (Fig. 3). Comparison between the tectonic maps of northwestern and southwestern Taiwan suggests that the reactivated normal fault in the foreland basin would influence the orientation of the tear faults in the inner fold-and-thrust belt and determine how the low-angle thrusts are segmented.

5.b. Possible mechanical conditions for normal fault reactivation

The tectonic map (Fig. 2) and seismic sections (Figs 6, 7) of northwestern Taiwan also show that not all the normal faults were reactivated, indicating that normal fault reactivation is a highly selective process;

https://doi.org/10.1017/S0016756816000637 Published online by Cambridge University Press

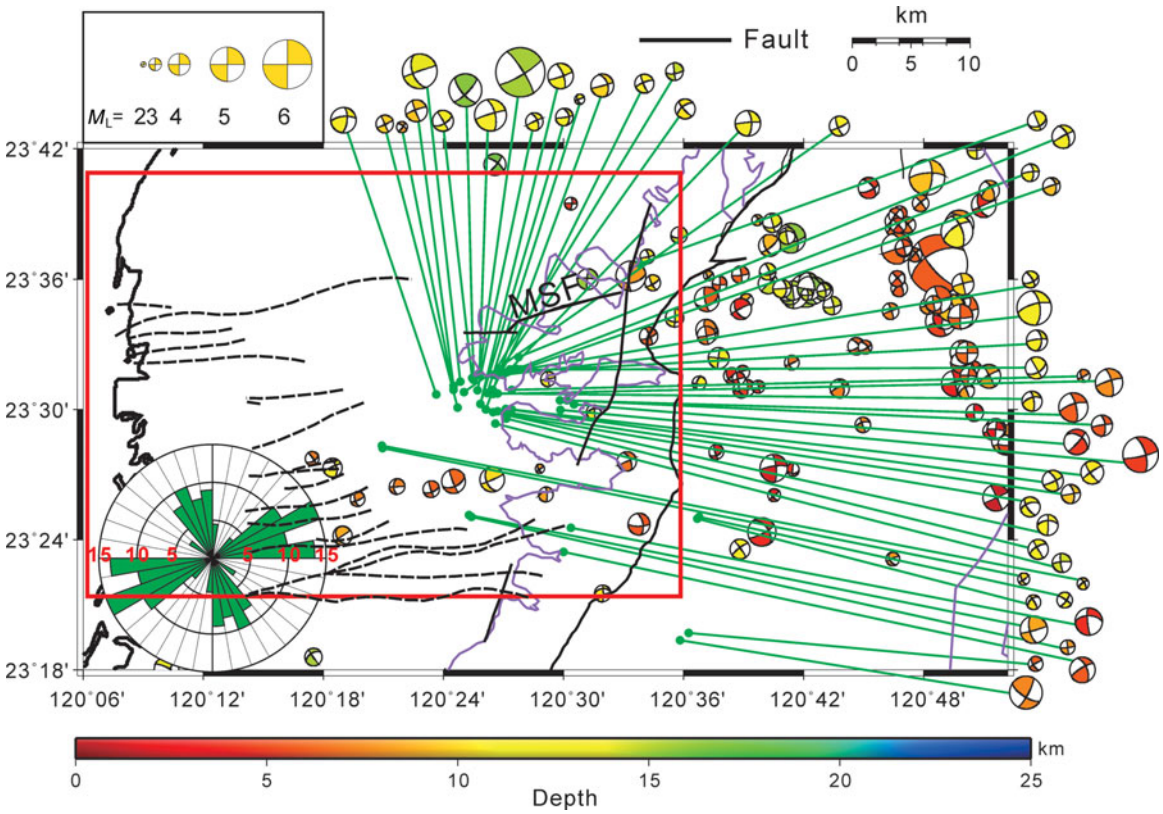

Figure 19. Distribution of strike-slip fault plane solutions in onshore southwestern Taiwan and a rose diagram showing the main trend of the fault planes in the Meishan area (red frame). One set of the fault planes is trending ENE–WSW, parallel to that of the Meishan fault.

those faults that were reactivated are dipping to the south, the orientation being optimum for the normal faults to be reactivated under the condition of northwestwards vergence of contractional deformation. The Hsinchu fault may be the only exception (see description of the fault in Section 3.b.1). However, this factor is not the only reason for the normal fault to be reactivated; we also observe that many normal faults that are dipping to the south are not reactivated in the offshore and outer fold-and-thrust belt (Figs 5, 7). Sibson (1985, 1995) predicts that, for a certain internal friction coefficient, the range of dip angles for the normal fault to be reactivated is limited. It is around <50°, and any normal faults with a larger dip angle would not be reactivated under any conditions unless the internal friction coefficient of rock or fault zone decreases. If the strike of the normal fault is not perpendicular to that of the maximum horizontal stress, such as the situation in northwestern Taiwan, diagrams of variations in internal friction coefficient and relative angle between normal fault plane and stress axes (as proposed by Sassi *et al.* 1993) can be used to predict structural characters of the reactivated normal fault. The relative angle between normal fault plane, with 60° dip in average, and maximum horizontal stress in northwestern Taiwan can be plotted in such diagrams; the results indicate that only those normal faults with an internal friction angle of <20° of fault plane could be reactivated with dextral strike-slip component.

5.c. Definition of deformation front of orogenic belt

As reactivated normal faults are quite common in northwestern Taiwan, the deformation front in this part of orogenic belt cannot be clearly classified as any of the types proposed by Morley (1986). Mouthereau *et al.* (2002) proposed a reactivation front that marks the boundary of appearance of the reactivated normal faults in an offshore area and gave another definition for the deformation front based on mechanics viewpoint. They drew a highly curved reactivation front in the western margin of the Taishih Basin. From a long-term deformation point of view, we would maintain the definition of deformation front *sensu stricto* to describe the boundary of the orogenic belt. We suggest that, because the reactivated normal faults have been involved in the outer fold-and-thrust belt, the deformation front in onshore northwestern Taiwan is a wide zone rather than a boundary that can be defined by any specific major thrusts. As for the reactivated normal faults in the offshore area, their formation can be attributed to far-field stress transmitted into the foreland basin.

In southwestern Taiwan, the deformation front can be marked along the western limb of the fold structures that are located right next to the frontal thrusts of the fold-and-thrust belt. These fold structures also cover the exposed active faults on the surface (Fig. 3). The difference in the characteristics of deformation fronts in the two foreland areas is basically due to the contrast in structural style of normal fault reactivation.

https://doi.org/10.1017/S0016756816000637 Published online by Cambridge University Press

5.d. Contrast in structural style of normal fault reactivation

The tectonic maps (Figs 1–3) show significant difference in normal fault reactivation in the offshore and coastal plain of southwestern Taiwan in that none of the normal faults (except the Meishan active fault) has been reactivated, in contrast to that in northwestern Taiwan. Seismic sections located on the front of the fold-and-thrust belt in southwestern Taiwan show that all the high-angle faults still display normal offsets and that the foreland basin strata thicken and tilt up towards the frontal thrust (Fig. 18b–d). This monocline structure has been ascribed to a buried thrust with forelandwards vergence underneath the Neogene strata (Yang, 2007), which cannot be observed in the seismic sections and is not likely to create the structure with hinterlandwards vergence. The structural feature can be viewed as an inverted structure and its trend is parallel to that of the fold-and-thrust belt or the overprinted Palaeogene normal faults, not with that of the pre-existing Neogene normal faults. We speculate that it could be caused by reactivation of another set of normal faults in the deeper part of the basement, which cannot be identified in the seismic sections, or simply by 'basement folding' (Bellahsen *et al.* 2012). However, this might be the only clue indicating that the Palaeogene extensional tectonic settings are involved in the foreland tectonics.

The contrast in foreland tectonics in different segments of the fold-and-thrust belt also provides some important clues to test tectonic models relating orogenic modes (thin-skinned v. thick-skinned models) with the crustal/lithospheric strength (as reflected by the equivalent elastic thickness). Mouthereau & Petit (2003) proposed that, taking the Taiwan orogenic belt as an example, low crustal/lithospheric strength would have favoured thick-skinned deformation. In their model, the lower crustal/lithospheric strength also corresponds to the higher curvature of the reactivation front in offshore southwestern Taiwan and thick-skinned deformation is manifested by a thicker seismogenic zone in the crust, which corresponds to more numerous reactivated normal faults. Alternatively, Butler, Tavarnelli & Grasso (2006) proposed that it is the relative strength between the pre-existing normal fault and the crust that determines whether the pre-existing normal faults are easily reactivated; in the situation of relative weaker crust, 'pre-existing faults may have served to create initial perturbation upon which large-scale interfacial buckles nucleated' and 'the surrounding basement rocks are deformed' (Butler, Tavarnelli & Grasso, 2006).

The equivalent elastic thickness, estimated by flexural modelling of the foreland basin in western Taiwan, indicates that the crust/lithosphere is weaker in the southwestern part than that in the northwestern part of Taiwan foreland (Lin & Watts, 2002; Mouthereau & Petit, 2003). In response to the weaker crust/lithosphere of southwestern Taiwan, the basement is deformed while the pre-existing basement-involved normal faults remain non-reactivated; only a segment with limited length along a normal fault is reactivated (Fig. 18b–d). What we observed and described in southwestern Taiwan suggests that the deforming basement rocks in a weaker crust/lithosphere would respond to the tectonic stress in the foreland and prevent the basement-involved normal faults from being reactivated. As for those reactivated normal faults in northwestern Taiwan, mechanical analysis based on the theories of Sibson (1985, 1995) and Sassi *et al.* (1993) described in Section 5.b suggests a lower internal friction coefficient for a pre-existing normal fault plane. We suggest that these normal faults embedded in stronger crust would be easier to be reactivate than those in southwestern Taiwan.

5.e. Implications of normal fault reactivation in active tectonics

The examples of active faults that we present in this paper occur in different parts of the fold-and-thrust belt (Figs 10c, 11c, 13b, 18) and are related to reactivated basement-involved normal faults trending obliquely to the front of the orogen. Although the main shocks of historical earthquakes occurring on these fault planes vary in fault type and orientation (Figs 2, 3) –those in the inner fold-and-thrust belt are characterized by thrust faults trending parallel to the surface major thrusts – the fault plane solutions of the main shocks in the outer fold-and-thrust belt and coastal plain indicate strike-slip faults trending ENE–WSW. In the former situation, the shallow part of the pre-existing normal fault acts passively as a ramp of the low-angle major thrust and the fault plane solutions reflect the long-term orientation of slip along the low-angle thrust. Active faults in the outer fold-and-thrust belt and coastal plain are likely truly reactivated normal faults that actively deform in response to the regional collisional stress. We may therefore classify normal fault reactivation into active and passive types, which play different roles in the deformation of the foreland tectonics in western Taiwan.

6. Conclusions

Basement-involved pre-existing normal faults play important but various roles in the different parts of the Taiwan fold-and-thrust belt and create various structural styles. In offshore northwestern Taiwan, long reactivated normal faults with a strike-slip component have developed by linkage of reactivated single pre-existing normal faults in the foreland basin. The reactivated normal faults extend into the onshore outer fold-and-thrust belt and play the roles of transverse structures in the development of low-angle thrusts. The length of the low-angle thrusts is confined by the transverse structures, which formed a tear fault or lateral ramp for the terminated thrusts. At a later stage, the transverse structures were overthrust and appear underneath the low-angle thrust or became ENE–WSW-trending tear faults in the inner fold-and-thrust belt.

https://doi.org/10.1017/S0016756816000637 Published online by Cambridge University Press

In southwestern Taiwan, where the foreland basin is almost devoid of reactivated normal faults, the pre-existing normal faults also influenced the development of the geometry of low-angle thrust in the outer fold-and-thrust belt; the shallow parts of pre-existing normal faults, acting passively as a ramp for the low-angle thrusts when the major thrusts propagated forelandwards, stepped up along the normal fault plane and cut upwards to the surface. The way the pre-existing normal faults involved in the inner fold-and-thrust belt also results in a WNW–ESE-trending tear fault in the belt, different from that in northwestern Taiwan.

The deformation front *sensu stricto* in onshore northwestern Taiwan is now around the coastal line and is a wide zone rather than a boundary that can be defined by any specific major thrust. In contrast to that, the deformation front in the foreland basin of onshore southwestern Taiwan can be marked along the western limb of the monoclonal structures that are located right next to the frontal thrusts of the outer fold-and-thrust belt.

Some of the faults active today in western Taiwan may be related to the reactivated normal faults which, with right-lateral slip component, occur in the frontal area of the fold-and-thrust belt or even beneath the low-angle thrusts. These active faults have similar structural trends as those formed during the regional extensional tectonics. Some of the earthquake main shocks, with hypocentres in the footwall of the low-angle thrust, reveal thrust types of fault plane solutions. The hypocentres of these major earthquakes can however be located on the pre-existing normal fault planes. The fact that these normal faults act as a high-angle ramp for the major thrusts implies a relationship between the existence of the normal fault and the triggering of the recent major earthquakes.

The lack of a reactivated normal fault in southwestern Taiwan, where the basement has been regarded weaker than that in northwestern Taiwan, may suggest that a weaker crust would respond to the tectonic stress by taking most of the deformation in the foreland and prevent the basement-involved normal faults from being reactivated. In contrast, normal faults embedded in stronger crust as in northwestern Taiwan would be easier to reactivate than those in southwestern Taiwan.

Acknowledgements. The authors would like to thank Exploration and Development Research Institute, CPC Corporation, Taiwan for providing invaluable well-bore and seismic data and their long-term support of this study. The authors would also like to thank Dr Chih-Wei Chien, Ms E.-Wen Cheng, Mr Tzu-Ruei Yang and Mr Chia-Hsun Yang from the Department of Earth Sciences, National Cheng Kung University for preparing the figures and editing the text. Special thanks are extended to Drs Brown and Lacombe for their invaluable comments and suggestions. The research results reported here are part of the projects MOST 103-3113-E-006-012 and MOST 105-2119-M-865-002, supported by the Ministry of Science and Technology of Taiwan Government, and FED0111001, supported by Exploration and Development Research Institute, CPC Corporation, Taiwan.

References

Alvarez-Marron, J., Brown, D., Camanni, G., Wu, Y.-M. & Kuo-Chen, Z. H. 2014. Structural complexities in a foreland thrust belt inherited from the shelf-slope transition: Insights from the Alishan area of Taiwan. *Tectonics* **33**, 1322–39.

Amilibia, A., McClay, K. R., Sàbat, F., Muñoz, J. A. & Roca, E. 2005. Analogue modelling of inverted oblique rift systems. *Geologica Acta* **3**, 251–71.

Bellahsen, N., Jolivet, L., Lacombe, O., Bellanger, M., Boutoux, A., Garcia, S., Mouthereau, F., Le Pourhiet, L. & Gumiaux, C. 2012. Mechanisms of margin inversion in the external Western Alps: Implications for crustal rheology. *Tectonophysics* **560–1**, 62–83.

Beyssac, O., Simoes, M., Avouac, J. P., Farley, K. A., Chen, Y.-G., Chan, Y.-C. & Goffé, B. 2007. Late Cenozoic metamorphic evolution and exhumation of Taiwan. *Tectonics* **26**, TC6001, 32 pp.

Biq, C. C. 1972. Duel-trench structure in theTaiwan-Luzon region. *Proceedings of the Geological Society of China* **15**, 65–75.

Biq, C. C. 1992. Another coastal range on Taiwan. *Ti-Chih* **12**, 1–14 (in Chinese).

Brown, D., Alvarez-Marron, J., Schimmel, M., Wu, Y.-M. & Camanni, G. 2012. The structure and kinematics of the central Taiwan mountain belt derived from geological and seismicity data. *Tectonics* **31**, TC5013, 25 pp.

Brown, W. G. 1984. *Basement Involved Tectonics Foreland Areas*. American Association of Petroleum Geologists, Tulsa, Continuing Education Course Note Series #26, 92 pp.

Buchanan, J. G. & Buchanan, P. G. 1995. *Basin Inversion*. Geological Society of London. Geological Society Special Publications no.88, 596 pp.

Butler, R. W. H., Tavarnelli, E. & Grasso, M. 2006. Structural inheritance in mountain belts: an Alpinee–Apennine perspective. *Journal of Structural Geology* **28**, 1893–908.

Carola, E., Tavani, S., Ferrer, O., Granado, P., Quinta, A., Butillé, & Muñoz, J. A. 2013. Along-strike extrusion at the transition between thin- and thick-skinned domains in the Pyrenean Orogen (northern Spain). In *Thick-Skin-Dominated Orogens: From Initial Inversion to Full Accretion* (eds M. Nemčok, A. Mora & W. Cosgrove), pp. 119–40. Geological Society of London, Special Publication no. 377.

Carrera, N. & Muñoz, J. A. 2013. Thick-skinned tectonic style resulting from the inversion of previous structures in the southern Cordillera Oriental (NW Argentine Andes). In *Thick-Skin-Dominated Orogens: From Initial Inversion to Full Accretion* (eds M. Nemčok, A. Mora & W. Cosgrove), pp.77–100. Geological Society of London, Special Publication no. 377.

Chai, B. H. T. 1972. Structural and tectonic evolution of Taiwan. *American Journal of Science* **272**, 389–422.

Chang, Y. L., Lee, C. I., Lin, C. U., Hsu, C. H. & Mao, E. W. 1996. Inversion tectonics in the fold-thrust belt of the foothills of Chiayi-Tainan area, southwestern Taiwan. *Petroleum Geology of Taiwan* **30**, 163–76.

Cheng, S. N. 1995. The study of stress distribution in and around Taiwan. Ph.D. Thesis, National Central University, Chungli, Taiwan. Published thesis.

Chi, W. R., Namson, J. & Suppe, J. 1981. Record of plate interactions in the Coastal Range, Eastern Taiwan. *Memoir of Geological Society of China* **4**, 155–94.

CHINESE PETROLEUM CORPORATION. 1978. Geologic Map of Western Taiwan, Taoyuan-Hsinchu Sheet (1:100000). TPED, CPC, Miaoli, Taiwan.

CHINESE PETROLEUM CORPORATION. 1986. Geologic Map of Western Taiwan, Chiayi Sheet (1:100000). TPED, CPC, Miaoli, Taiwan.

CHINESE PETROLEUM CORPORATION. 1989. Geologic Map of Western Taiwan, Tainan Sheet (1:100000). TPED, CPC, Miaoli, Taiwan.

CHINESE PETROLEUM CORPORATION. 1992. Geologic Map of Western Taiwan, Kaohsiung Sheet (1:100000). TPED, CPC, Miaoli, Taiwan.

CHINESE PETROLEUM CORPORATION. 1994. Geologic Map of Western Taiwan, Miaoli Sheet (1:100000). TPED, CPC, Miaoli, Taiwan.

CHIU, H. T. 1970. Structural features of the area between Hsinchu and Taoyuan, northern Taoyuan, northern Taiwan. *Proceedings of the Geological Society of China* **13**, 63–75.

CHIU, H. T. 1971. Folds in the northern half of western Taiwan. *Petroleum Geology of Taiwan* **8**, 7–19.

CHOW, J., YANG, K.-M. & CHEN, H. M. 1987. Structural traps of the Paiho area, Southern Taiwan. *Petroleum Geology of Taiwan* **23**, 13–39.

CHOW, J., YANG, K.-M. & CHEN, H. M. 1988. Seismic interpretation of the Subsurface strutures in the Yuchu-Chiali area, Southern Taiwan. *Petroleum Geology of Taiwan* **24**, 60–95.

CHOW, J., YUAN, J. & YANG, K.-M. 1986. Geological interpretation of the seismic in the Houpi area, Taiwan. *Petroleum Geology of Taiwan* **22**, 27–53.

CHUANG, R. Y., JOHNSON, K. M., WU, Y.-M., CHING, K.-E. & KUO, L.-C. 2013. A midcrustal ramp-fault structure beneath the Taiwan tectonic wedge illuminated by the 2013 Nantou earthquake series. *Geophysical Research Letters* **40**, 5080–4.

COHEN, C. 1982. Model for a Passive to Active Continental Margin Transition: Implications for Hydrocarbon Exploration. *Association of Petroleum Geologists Bulletin* **66**, 708–18.

COOPER, M. S. & WILLIAMS, G. D. (eds) 1989. *Inversion Tectonics*. Blackwell Scientific Publications, Geological Society Special Publication No. 44, 375 pp.

COVEY, M. 1984. Lithofacies analysis and basin reconstruction, Plio-Pleistocene western Taiwan foredeep. *Petroleum Geology of Taiwan* **20**, 53–83.

COWARD, M. P. 1994. Inversion tectonics. In *Continental Deformation* (ed. P. I. Hancock), pp. 289–304. Oxford: Pergamon Press.

DUNNE, W. M. & FERRILL, D. A. 1988. Blind thrust systems. *Geology* **16**, 33–6.

EISENSTADT, G. & WITHJACK, M. O. 1995. Estimating inversion: results from clay models. In *Basin Inversion* (eds J. G. Buchanan & P. G. Buchanan), pp. 119–36. Geological Society of London, Special Publication no. 88.

ETHERIDGE, M. A., BRANSON, J. C. & STUART-SMITH, P. G. 1985. Extensional basin-forming structures in Bass strait and their importance for hydrocarbon exploration. *Australian Petroleum Exploration Association Journal* **25**, 344–61.

FUH, S. C. 2000. Magnitude of Cenozoic erosion from mean sonic transit time, offshore Taiwan. *Marine and Petroleum Geology* **17**, 1011–28.

HARDING, T. P. & TUMIMAS, A. C. 1988. Interpretation of footwall (lowside) fault traps sealed by reverse faults and convergent wrench faults. *American Association of Petroleum Geologists Bulletin* **72**, 738–57.

HICKMAN, J. B., WILTSCHKO, D. V., HUNG, J. H., FANG, P. & BOCK, Y. 2002. Structure and evolution of the active fold-and-thrust belt of southwestern Taiwan from Global Positioning System analysis. In *Geology and Geophysics of an Arc-Continent Collision* (eds T.B. Byrne & C.-S. Liu), pp. 75–92. Geological Society of America, Colorado, Special Papers no. 358.

HO, C. S. 1982. *Tectonic Evolution of Taiwan: Explanatory Text of the Tectonic Map of Taiwan*. Central Geological Survey, MOEA, Taipei, 126 pp.

HO, C.-S. 1986. *An Introduction to the Geology of Taiwan: Explanatory Text of the Geologic Map of Taiwan*. Central Geological Survey, MOEA, Taipei, 153 pp.

HSIAO, P. T. 1974. Subsurface geologic study of the Hsinying Coastal area, Taiwan. *Petroleum Geology of Taiwan* **11**, 27–39.

HUANG, C.-Y., WU, W.-Y., CHANG, C.-P., TSAO, S., YUAN, P. B., LIN, C.-W. & XIA, K.-Y. 1997. Tectonic evolution of accretionary prism in the arc-continent collision terrane of Taiwan. *Tectonophysics* **281**, 31–51.

HUANG, C.-Y., YUAN, P. B. & TSAO, S.-J. 2006. Temporal and spatial records of active arc-continent collision in Taiwan: A synthesis. *Geological Society of America Bulletin* **118**, 274–88.

HUANG, C.-Y., XIA, K., YUAN, P. B. & CHEN, P.-G. 2001. Structural evolution from Paleogene extension to Latest Miocene-Recent arc-continent collision offshore Taiwan: comparison with on land geology. *Journal of Asian Earth Sciences* **19**, 619–39.

HUANG, F. F. W. 1986. Controlling factors for hydrocarbon accumulation in the Talu "sands" of northwestern Taiwan. *Petroleum Geology of Taiwan* **22**, 1–18.

HUANG, F. F. W. 1987. Wrench faults in western Taiwan and oil-gas accumulation. *Petroleum Geology of Taiwan* **23**, 1–12.

HUANG, S. L. 2009. The transition of structural style in the foothills in Chiayi area, southern Taiwan. M.Sc. thesis, Department of Geosciences, National Taiwan University, Taipei, Taiwan. Published thesis.

HUANG, S. T., CHEN, R. C. & CHI, W. R. 1993. Inversion tectonics and evolution of the northern Taihsi Basin, Taiwan. *Petroleum Geology of Taiwan* **28**, 15–46.

HUANG, T. Y. 1967. Foraminiferal study of the Tungliang Well TL-1 of the Penghu Islands. *Petroleum Geology of Taiwan* **5**, 131–49.

HUNG, J. H. & SUPPE, J. 2002. Subsurface geometry of the Sani–Chelungpu faults and fold scarp formation in the 1999 Chi-Chi Taiwan Earthquake. AGU 2002 Fall Meeting. 6–10 December 2002, San Franciso.

HUNG, J. H. & WILTSCHKO, D. V. 1993. Structure and kinematics of arcuate thrust faults in the Miaoli-Cholan area of western Taiwan. *Petroleum Geology of Taiwan* **28**, 59–96.

HUNG, J. H., WILTSCHKO, D. V., LIN, H. C., HICKMAN, J. B., FANG, P. & BOCK, Y. 1999. Structure and motion of the southwestern Taiwan fold and thrust Belt. *Terrestrial Atmospheric and Oceanic Sciences* **10**, 543–68.

JACKSON, J. A. 1980. Reactivation of basement faults and crustal shortening in orogenic belts. *Nature* **343**, 343–6.

JAHN, B. M., CHI, W. R. & YUI, T. F. 1992. A late Permian formation of Taiwan (marbles from Chia-Li Well no. 1): Pb-Pb isochron and Sr isotopic evidence, and its regional geological significance. *Journal of the Geological Society of China* **35**, 193–218.

JIMENEZ, L., MORA, A., CASALLAS, W., SILVA, A., TESÓN, E., TAMARA, J., NAMSON, J., HIGUERA-DÍAZ, I. C., LASSO, A. & STOCKLI, D. 2013. Segmentation and growth of foothill thrust-belts adjacent to inverted grabens: the

case of the Colombian Llanos foothills. In *Thick-Skin-Dominated Orogens: From Initial Inversion to Full Accretion* (eds M. Nemčok, A. Mora & W. Cosgrove), pp. 189–220. Geological Society of London, Special Publication no. 377.

KELLER, J. V. A. & MCCLAY, K. R. 1995. 3D sandbox models of positive inversion. In *Basin Inversion* (eds J. G. Buchanan & P. G. Buchanan), pp. 137–46. Geological Society of London, Special Publication no. 88.

LACOMBE, O. & MOUTHEREAU, F. 2002. Basement-involved shortening and deep detachment tectonics in forelands of orogens: Insights from recent collision belts (Taiwan, Western Alps, Pyrenees). *Tectonics* **21**(4) 1030, 12.1–22.

LACOMBE, O., MOUTHEREAU, F., ANGELIER, J., CHU, H.-T. & LEE, J. C. 2003. Frontal belt curvature and oblique ramp development at an obliquely collided irregular margin: geometry and kinematics of the NW Taiwan fold-thrust belt. *Tectonics* **22**(3) 1025, 9.1–16.

LACOMBE, O., MOUTHEREAU, F., ANGELIER, J. & DEFFONTAINES, B. 2001. Structural, geodetic and seismological evidence for tectonic escape in SW Taiwan. *Tectonophysics* **333**, 323–45.

LEE, C. I., CHANG, Y. L. & COWARD, M. P. 2002. Inversion tectonics of the fold-and-thrust belt, western Taiwan. In *Geology and Geophysics of an Arc-Continent Collision, Taiwan* (eds T. B. Byrne & C. S. Liu), pp. 13–30. Geological Society of America, Boulder, Special Paper no. 358.

LEE, C. I., CHANG, Y. L., MAO, E. W. & TSENG, C. S. 1993. Fault reactivation and structural inversion in the Hsinchu-Miaoli area of northern Taiwan. *Petroleum Geology of Taiwan* **28**, 47–58.

LEE, Y.-H., BYRNE, T., WANG, W.-H., LO, W., RAU, R.-J. & LU, H.-Y. 2015. Simultaneous mountain building in the Taiwan orogenic belt. *Geology* **43**, 451–54.

LETOUZEY, J. 1986. Cenozoic paleostress pattern in the Alpine Foreland and structural interpretation in a platform basin. *Tectonophysics* **132**, 215–31.

LEU, R. T., CHIANG, C. L. & HUANG, F. W. F. 1985. Study on the Pachangchi structure, Chaiyi, Taiwan. *Petroleum Geology of Taiwan* **21**, 13–32.

LIN, A. T. & WATTS, A. B. 2002. Origin of the West Taiwan basin by orogenic loading and flexure of a rifted continental margin. *Journal of Geophysical Research* **107**(B9), 2185, ETG 2-1–19.

LIN, A. T., WATTS, A. B. & HESSELBO, S. P. 2003. Cenozoic stratigraphy and subsidence history of the South China Sea margin in the Taiwan region. *Basin Research* **15**, 453–78.

LIN, C. W., CHANG, H. C., LU, S. T., SHIH, T. S. & HUANG, W. J. 2000. *An Introduction to the Active Faults of Taiwan (With Explanatory Text of the Active Fault Map of Taiwan, Scale 1:500,000)*. Special Publication of the Central Geological Survey no. 13, 122 pp. MOEA ROC (in Chinese).

LIN, D. H., CHEN, K. H., RAU, R. J. & HU, J. C. 2013. The role of a hidden fault in stress triggering: Stress interactions within the 1935 *Mw* 7.1 Hsinchu-Taichung earthquake sequence in central Taiwan. *Tectonophysics* **601**, 37–52.

LIN, Y. N. 2005. Surface deformation and seismogenic structure model of the 1935 Hsinchu-Taichung earthquake (M_{GR}=7.1), in Miaoli, northwestern Taiwan. M.Sc. thesis, Department of Geosciences, National Taiwan University, Taipei, Taiwan. Published thesis.

LU, C. Y. 1994. Neotectonics in the foreland thrust belt of Taiwan. *Petroleum Geology of Taiwan* **29**, 1–26.

LU, C. Y., JENG, F. S., CHANG, K. J. & JIAN, W. T. 1998. Impact of basement high on the structure and kinematics of the western Taiwan. *Terrestrial Atmospheric and Oceanic Sciences* **9**, 533–50.

LU, C. Y. & MALAVIEILLE, J. 1994. Oblique convergence, indentation and rotation tectonics in the Taiwan mountain belt: Insights from experimental modeling. *Earth and Planetary Science Letters* **121**, 477–94.

MACEDO, J. & MARSHAK, S. 1999. Controls on the geometry of fold-thrust belt salients. *Geological Society of America Bulletin* **111**(12), 1808–22.

MARSHAK, S. 2004. Salients, recesses, arcs, oroclines, and syntaxes: A review of ideas concerning the formation of map-view curves in fold-thrust belts. In *Thrust Tectonics and Hydrocarbon Systems* (ed. K. R. McClay), pp. 131–56. American Association of Petroleum Geologists, Tulsa, Memoir no. 82.

MENG, C. Y. 1962. Wrench fault tectonism in Taiwan and its relations to the petroleum potentialities. *Petroleum Geology of Taiwan* **1**, 1–22.

MENG, C. Y. 1967. The structural development of the southern half of western Taiwan. *Proceedings of the Geological Society of China* **10**, 77–82.

MESALLES, L., MOUTHEREAU, F., BERNET, M., CHANG, C.-P., LIN, A.T., FILLON, C. & SENGELEN, X. 2014. From submarine continental accretion to arc-continent orogenic evolution: the thermal record in southern Taiwan. *Geology* **42**, 907–10.

MORENO, N., SILVA, A., MORA, A., TESÓN, E., QUINTERO, I., ROJAS, L. E., LOPEZ, C., BLANCO, V., CASTELLANOS, J., SANCHEZ, J., OSORIO, L., NAMSON, J., STOCKLI, D. & CASALLASW, W. 2013. Interaction between thin- and thick-skinned tectonics in the foothill areas of an inverted graben. The Middle Magdalena Foothill belt. In *Thick-Skin-Dominated Orogens: From Initial Inversion to Full Accretion* (eds M. Nemčok, A. Mora & W. Cosgrove), pp. 221–55. Geological Society of London, Special Publication no. 377.

MORLEY, C. K. 1986. A classification of thrust fronts. *American Association of Petroleum Geologists Bulletin* **70**, 12–25.

MOUTHEREAU, F., ANGELIER, J. & LEE, J. C. 2001. Le séisme du 21 Septembre 1999: influence de l'héritage structural et implication du socle au front de la chaîne de Taiwan. *Compte Rendu Academy de Science Paris* **333**, 93–103.

MOUTHEREAU, F., DEFFONTAINES, B., LACOMBE, O. & ANGELIER, J. 2002. Variations along the strike of the Taiwan thrust belt: Basement control on structural style, wedge geometry, and kinematics. In *Geology and Geophysics of an Arc-continent Collision, Taiwan* (eds T. B. Byrne & C. S. Liu), pp. 31–54. Geological Society of America, Boulder, Special Paper no. 358.

MOUTHEREAU, F. & LACOMBE, O. 2006. Inversion of the Paleogene Chinese continental margin and thick-skinned deformation in the Western Foreland of Taiwan. *Journal of Structural Geology* **28**, 1977–93.

MOUTHEREAU, F., LACOMBE, O., DEFFONTAINES, B., ANGELIER, J. & BRUSSET, S. 2001. Deformation history of the southwestern Taiwan foreland thrust belt: insights from tectono-sedimentary analyses and balanced cross-sections. *Tectonophysics* **333**, 293–318.

MOUTHEREAU, F. & PETIT, C. 2003. Rheology and strength of the Eurasian continental lithosphere in the foreland of the Taiwan collision belt: Constraints from seismicity, flexure, and structural styles. *Journal of Geophysical Research* **108** (B11), 2512, ETG 1-1–1-15.

MOUTHEREAU, F., WATTS, A. B. & BUROV, E. 2013. Structure of orogenic belts controlled by lithosphere age. *Nature Geoscience* **6**, 785–89.

NAMSON, J. 1981. Detailed structural analysis of the western foothills belt in the Miaol-Hsinchu area, Taiwan: (I) southern part. *Petroleum Geology of Taiwan* **18**, 31–51.

NAMSON, J. 1983. Structure of the western foothills belt, Miaoli-Hsinchu area, Taiwan: (II) central part. *Petroleum Geology of Taiwan* **19**, 51–76.

NAMSON, J. 1984. Structure of the western foothills belt, Miaoli Hsinchu area, Taiwan: (III) northern part. *Petroleum Geology of Taiwan* **20**, 35–52.

NEMČOK, M., MORA, A. & COSGROVE, J. 2013. Thick-skin-dominated orogens; from initial inversion to full accretion: an introduction. In *Thick-Skin-Dominated Orogens: From Initial Inversion to Full Accretion* (eds M. Nemčok, A. Mora & J. Cosgrove), pp. 1–17. Geological Society of London, Special Publication no. 377.

RAU, R. J. & WU, F. T. 1995. Tomographic imaging of lithospheric structures under Taiwan. *Earth and Planetary Science Letters* **133**, 517–32.

RAU, R. J., WU, F. T. & SHIN, T. C. 1996. Regional network focal mechanism determination using 3-D velocity model and SH/P amplitude ratio. *Bulletin of the Seismological Society of America* **86**, 1270–83.

SASSI, W., COLLETTA, B., BALE, P. & PAQUEREAU, T. 1993. Modelling of structural complexity in sedimentary basins: The role of pre-existing faults in thrust tectonics. *Tectonophysics* **226**, 97–112.

SENGOR, A. M. C. 1976. Collision of irregular continental margins: Implications for foreland deformation of Alpine-type orogens. *Geology* **4**, 779–82.

SENGOR, A. M. C., BURK, K. & DEWEY, J. F. 1978. Rift at high angles to orogenic belts: Tests for their origin and the upper Rhine graben as an example. *American Journal of Sciences* **278**, 24–40.

SENO, T. 1977. The instantaneous rotation vector of the Philippine Sea Plate relative to the Eurasian Plate. *Tectonophysics* **42**, 209–26.

SENO, T., STEIN, S. & GRIPP, A. E. 1993. A model for the motion of the Philippine Sea Plate consistent with NUVEL-1 and geological data. *Journal of Geophysical Research: Solid Earth* **98**(B10), 17941–48.

SHEU, H. C., KOSUGA, M. & SATO, H. 1982. Mechanism and fault model of the Hsinchu–Taichung (Taiwan) earthquake of 1935. *Zisin* **2**, 567–74 (in Japanese).

SIBSON, R. H. 1985. A note on fault reactivation. *Journal of Structural Geology* **7**, 751–4.

SIBSON, R. H. 1995. Selective fault reactivation during basin inversion: potential for fluid redistribution through fault-valve action. In *Basin Inversion* (eds J. G. Buchanan & P. G. Buchanan), pp. 3–19. Geological Society of London, Special Publication no. 88.

SIBUET, J.-C. & HSU, S.-K. 1997. Geodynamics of the Taiwan arc-arc collision. *Tectonophysics* **274**, 221–51.

SINCLAIR, I. K. 1995. Transpressional inversion due to episodic rotation of extensional stress in Jeanne d'Arc Basin, offshore Newfoundland. In *Basin Inversion* (eds J. G. Buchanan & P. G. Buchanan), pp. 249–71. Geological Society of London, Special Publication no. 88.

SUN, S. C. 1982. The Tertiary basins of offshore Taiwan. *Proceedings of the Second ASCOPT Conference and Exhibition*, Manila, Philippines, 126–35.

SUPPE, J. 1976. Décollement folding in southwestern Taiwan. *Petroleum Geology of Taiwan* **13**, 25–35.

SUPPE, J. 1980. Imbricated structure of western foothills belt, southcentral Taiwan. *Petroleum Geology of Taiwan* **17**, 1–16.

SUPPE, J. 1981. Mechanics of mountain building and metamorphisms in Taiwan. *Memoir of Geological Society of China* **4**, 67–89.

SUPPE, J. 1984. Seismic interpretation of the compressively reactivated normal fault near Hsinchu, western Taiwan. *Petroleum Geology of Taiwan* **20**, 85–96.

SUPPE, J. 1985. *Principles of Structural Geology*. New Jersey: Prentice-Hall, 560 pp.

SUPPE, J. 1986. Reactivated normal faults in the western Taiwan fold-and-thrust belt. *Memoir of Geological Society of China* **7**, 187–200.

SUPPE, J. & NAMSON, J. 1979. Fault-bend origin of frontal folds of the western Taiwan fold and thrust belt. *Petroleum Geology of Taiwan* **16**, 1–18.

TANG, C.-H. 1977. Late Miocene erosional unconformity on the subsurface Peikang high beneath the Chiayi-Yunlin Coastal Plain, Taiwan. *Memoir of the Geological Society of China* **2**, 155–67.

TENG, L. S. 1990. Geotectonic evolution of late Cenozoic arc-continent collision in Taiwan. *Tectonophysics* **183**, 57–76.

TENG, L. S. & WANG, Y. 1981. Island arc system of the Coastal Range, eastern Taiwan. *Proceedings of the Geological Society of China* **24**, 99–112.

TENG, L. S., WANG, Y., TANG, C.-H., HUANG, C.-Y., HUANG, T.-C., YU, M.-S. & KE, A. 1991. Tectonic aspects of the Paleogene depositional basin of northern Taiwan. *Proceedings of the Geological Society of China* **34**, 313–35.

TESÓN, E., MORA, A., SILVA, A., NAMSON, J., TEIXELL, A., CASTELLANOS, J., CASALLAS, W., JULIVERT, M., TAYLOR, M., IBÁÑEZ-MEJÍA, M. & VALENCIA, V. A. 2013. Relationship of Mesozoic graben development, stress, shortening magnitude, and structural style in the Eastern Cordillera of the Colombian Andes. In *Thick-Skin-Dominated Orogens: From Initial Inversion to Full Accretion* (eds M. Nemčok, A. Mora & W. Cosgrove), pp. 257–83. Geological Society of London, Special Publication no. 377.

TSAI, Y. B. 1978. Plate subduction and the Plio-Pleistocene orogeny in Taiwan. *Petroleum Geology of Taiwan* **15**, 1–10.

VANN, I. R., GRAHAM, R. H. & HAYWARD, A. B. 1986. The structure of mountain fronts. *Journal of Structural Geology* **8**, 215–27.

WANG, C. Y., CHIEN, L. L., SU, F. C., LEU, M. T., WU, M. S., LAI, S. H. & CHERN, C. C. 2002. Structural mapping of the 1999 Chi-Chi earthquake fault, Taiwan, by seismic reflection methods. *Terrestrial Atmospheric and Oceanic Sciences* **13**, 211–26.

WELBON, A. I. & BUTLER, R. W. H. 1992. Structural styles in thrust belts developed through rift basins: a view from the western Alps. In *Structural and Tectonic Modeling and Its Application to Petroleum Geology* (eds R. M. Larsen, H. Brekke, B. T. Larsen & E. Talleraas), pp. 469–79. Norwegian Petroleum Society (NPF), Special Publication no. 1.

WU, Y. M., CHANG, C. H., ZHAO, L., SHYU, J. B. H., CHEN, Y. G., SIEH, K. & AVOUAC, J. P. 2007. Seismic tomography of Taiwan: Improved constraints from a dense network of strong-motion stations. *Journal of Geophysical Research* **112**, B08312.

YANG, C. C. B. 2007. Seismogenic structure of the Chiayi-Tainan Area and the long-term slip rates of frontal thrusts in southwestern Taiwan. Ph.D. thesis, Department of Geosciences, National Taiwan University, Taipei, Taiwan. Published thesis.

YANG, K. M., HUANG, S. T., WU, J. C., TING, H. H. & MEI, W. W. 2006. Review and new insights on foreland tectonics in western Taiwan. *International Geology Review* **48**, 910–41.

YANG, K. M., HUANG, S. T., WU, J. C., TING, H. H., MEI, W. W., LEE, M., HSU, H. H. & LEE, C. J. 2007. 3D geometry of the Chelungpu Thrust system in central Taiwan: Its implications for active tectonics. *Terrestrial, Atmospheric and Oceanic Sciences* **18**, 143–81.

YANG, K. M., TING, H. H., WU, J. C. & CHI, W. R. 1997. Geological model for complex structures and its implications for hydrocarbon exploration in northwestern Taiwan. *Petroleum Geology of Taiwan* **31**, 1–42.

YANG, K. M., TING, H. H. & YUAN, J. 1991. Structural styles and tectonic modes of Neogene extensional tectonics in southwestern Taiwan: Implications for hydrocarbon exploration. *Petroleum Geology of Taiwan* **26**, 1–31.

YANG, K. M., WU, J. C., CHENG, E. W., CHEN, Y. R., HUANG, W. C., TSAI, C. C., WANG, J. B. & TING, H. H. 2014. Development of tectonostratigraphy in distal part of foreland basin in southwestern Taiwan. *Journal of Asian Earth Sciences* **88**, 98–115.

YANG, K. M., WU, J. C., TING, H. H., WANG, J. B., CHI, W. R. & KUO, C. L. 1994. Sequential deformation in foothills belt, Hsinchu and Miaoli areas: Implications in hydrocarbon accumulation. *Petroleum Geology of Taiwan* **29**, 47–74.

YANG, K. M., WU, J. C., WICKHAM, J. S., TING, H. H., WANG, J. B. & CHI, W. R. 1996. Transverse structures in Hsinchu and Miaoli areas: structural mode and evolution in foothills belt, northwestern Taiwan. *Petroleum Geology of Taiwan* **30**, 111–50.

YUAN, J., YANG, K. M., CHI, W. R., HU, C. C. & CHOU, T. F. 1988. Episodic tectonism in the Tertiary continental margin of western Taiwan (abs). In *International Symposium on Geodynamic Evolution of Eastern Eurasian Margin*. 13–20 September 1988, Paris, France.

YUE, L. F., SUPPE, J. & HUNG, J. H. 2005. Structural geology of a classic thrust belt earthquake: the 1999 Chi-Chi earthquake Taiwan (M_w=7.6). *Journal of Structural Geology* **27**, 2058–83.

https://doi.org/10.1017/S0016756816000637 Published online by Cambridge University Press